ARCHIVE COPY

SHOCK STRUCTURE IN A PARTIALLY IONIZED GAS

by

Michel Y. Jaffrin

Fluid Mechanics Laboratory

Department of Mechanical Engineering
Massachusetts Institute of Technology

This research has been supported by the Advanced Research Projects Agency (Ballistic Missile Defense Office) and technically administered by the Fluid Dynamics Branch of the Office of Naval Research under Contract Nonr-1841(93).

October 1964

ERRATA

SHOCK STRUCTURE IN A PARTIALLY IONIZED GAS

Page	Line	Printed	Replace by
10	Eq (3 2)	$(\frac{c}{v})$	$(\frac{c^2}{v})$
22	Eq (4 8)	$3m_i(n'_{a_2} + n'_{i_2}) + m_e n'_{i_2}$	$3[m_i(n'_{a_2} + n'_{i_2}) + m_e n'_{i_2}]$
37	line (15)	(4 13), (4 10)	(4.14), (4 10)
42	last line	$n'_a T'^{3/4}_1$	$n'_{a_1} T'^{3/4}_1$
64	Table 2, ϕ_{max}	2 78 2 77	2 278 2 277
66	Fig. 2		delete a on horizontal scale

SHOCK STRUCTURE IN A PARTIALLY IONIZED GAS

Michel Y. Jaffrin

Department of Mechanical Engineering
Massachusetts Institute of Technology, Cambridge, Massachusetts

ABSTRACT

The one-dimensional, steady state structure of a shock wave in a partially ionized gas is investigated using the Navier-Stokes equations for the atom, electron, and ion fluids. The plasma is assumed quasi-neutral without a change in ionization across the shock. A characteristic feature common to weakly and strongly ionized gases is the existence of a broad layer of elevated electron temperature (thermal layer) ahead of the shock front due to the high electron thermal conductivity and of a precursor and an imbedded axial electric field induced by the charge separation. Because of the large atom-ion collision cross section due to the charge exchange mechanism, the ion slip is small when less than 30% of the plasma is ionized. In a weakly ionized plasma, the atom flow is unaffected by the ionized particles and the structure consists of an ordinary atom shock imbedded in the thermal layer. When the plasma is substantially ionized, the heavy particles are partially compressed and heated in the thermal layer and the ion and atom temperatures overshoot their downstream values in the shock. The induced electric fields increase with the degree of ionization and the

free stream Mach number while the shock thickness decreases. An experimental measurement in partially ionized hydrogen of the variation of potential in a strong shock gives a shock thickness and a potential rise across the imbedded shock in good agreement with the calculated values.

I. INTRODUCTION

While the study of a fully ionized plasma is relevant to astrophysical problems, it is more realistic to consider a partially ionized plasma in problems of re-entry physics and related laboratory experiments. The purpose of this work is to extend our solution for the shock structure in a fully ionized gas[1] to the case of a partially ionized gas, and to investigate the various plasma regimes leading to different types of shock structures. The shock structure in an ionized gas is complex and consists in general of a thin region in which most of the deceleration and heating of the flow occurs, imbedded within a much broader relaxation region. In our analysis, the term shock refers to the thin region while the broad relaxation region is termed a thermal layer.

Of particular interest in the present work is the study of the effects of the ion-atom diffusion or ion slip which is measured by the velocity and temperature differences between ions and atoms. The negative electric field induced by the charge separation inside the shock slows down the ions and creates an initial ion

---

1. M. Y. Jaffrin and R. F. Probstein, Phys. Fluids 7, Oct. (1964).

slip, which vanishes at the end of the shock after a sufficient number of ion-atom collisions.

As in our previous work, we seek the solution for a steady one-dimensional shock with no applied external electric or magnetic fields. The plasma is assumed here to be a ternary mixture of atoms, singly ionized ions, and electrons. The analysis is based on a three-fluid continuum approach using the Navier-Stokes equations as a model.

In order to make the problem mathematically tractable, we introduce three basic assumptions:

a. Frozen ionization: The increase in temperature across the shock produces further ionization of the gas following the shock, however, it is assumed that the characteristic chemical lengths are large compared to the shock thickness so that no ionization or recombination reactions take place in the shock itself.

b. Quasi-charge neutrality: It is assumed that the over all charge separation is negligible, a condition satisfied when the Debye length is much smaller than the mean free path, which is met for most plasmas.

c. Small ion slip: This follows from the fact that because of the large ion-atom cross section due to the charge exchange mechanism, the ion-atom mean free path ℓ_{ia_2} is in general small compared to the shock thickness Δ_s. As a result the ion slip, which is of the order of ℓ_{ia_2}/Δ_s, is small and may be computed by an iterative method.

The shock structure in a fully ionized gas has been investigated by several authors[1-4] but the case of a partially ionized gas has received less attention. Grewal and Talbot[5], assuming a Mott-Smith solution for the ions and atoms, and neglecting the ion slip found the existence of a broad thermal layer in front of the shock where the electron temperature rises. But they did not investigate the structure of the ion-atom shock and the assumption of small electron energy restricts their solution to the weakly ionized case. Pikel'ner[6] considered the inviscid transition region between a magnetohydrodynamic shock and the downstream state but he did not take into account the charge exchange mechanism which, by considerably increasing the atom-ion cross section, strongly inhibits the ion slip in the relaxation region.

II. BASIC EQUATIONS

There are for each type of particle, atom, ion, and electron the three continuum equations of mass, momentum, and energy. The electric field whose only non-zero component is E'_x is governed by Poisson's equation

---

2. J. D. Jukes, J. Fluid Mech. 3, 275 (1957)

3. V. D. Shafranov, Zh. Eksperim. i Teor. Fiz. 32, 1453 (1957) [Eng. Transl.: Soviet Phys. JETP 5, 1183 (1957)]

4. O. W. Greenberg, H. K. Sen, and Y. M. Treve, Phys. Fluids 3, 379 (1960)

5. M. S. Grewal and L. Talbot, J. Fluid Mech. 16, 573 (1963)

6. S. B. Pikel'ner, Zh. Eksperim. i Teor. Fiz. 36, 1536 (1959) [Eng. Transl.: Soviet Phys. JETP 7, 9 (1959)]

$$\frac{dE'_x}{dx'} = 4\pi e(n'_i - n'_e) \quad . \tag{2.1}$$

Here e is the magnitude of the electronic charge, x' the axial distance, and n' the number density; the subscripts i, e and a, denote ions, electrons and atoms respectively and the "primes" are used to distinguish the physical variables from the dimensionless variables which will be used later.

The net current j_x vanishes so that we have

$$j_x = 0 = (n'_i u'_i - n'_e u'_e)\, e$$

or

$$n'_i u'_i = n'_e u'_e \quad ,$$

where u' is the velocity. On integrating the steady one dimensional mass conservation equations for the ions and electrons, when there is no ionization or recombination, the constants of integration C_i and C_e are the same, giving:

$$n'_i u'_i = n'_e u'_e = C_i = C_e \quad . \tag{2.2}$$

The conservation of mass for atoms yields

$$n'_a u'_a = C_a \quad . \tag{2.3}$$

The constants of integration C_i and C_a are related to each other through the degree of ionization α. In the undisturbed plasma, all three species have the same mean velocity and the degree of ionization α can be expressed by the relation:

$$\alpha = \frac{n_i'}{n_i' + n_a'} = \frac{C_i}{C_i + C_a} \quad . \tag{2.4}$$

The conservation of momentum for the three species yields the following equations:

$$m_j C_j \frac{du_j'}{dx'} + \frac{dp_j'}{dx'} - \frac{d}{dx'}\left(\mu_j'' \frac{du_j'}{dx'}\right) - n_j' e_j E_x' = \sum_{k \neq j} P_{jk} \quad , \tag{2.5}$$

where m is the particle mass, μ'' the longitudinal coefficient of viscosity, p' the pressure and P_{jk} represents the longitudinal momentum transfer between species j and k and where j = i, e, a with the convention $e_i = +e$, $e_e = -e$, $e_a = 0$. The summation is made for $k \neq j$. The longitudinal coefficient of viscosity μ'' is related to the classical coefficient of viscosity μ by the relation

$$\mu'' = 4/3\ \mu \quad .$$

The corresponding energy equations are

$$\frac{5}{2}\frac{d}{dx'}(p_j'u_j') - \frac{d}{dx'}\left(\kappa_j \frac{dT_j'}{dx'}\right) - \frac{d}{dx'}\left(u_j'\mu_j'' \frac{du_j'}{dx'}\right) + \frac{m_j}{2} n_j'u_j' \frac{du_j'^2}{dx'}$$

$$-n_j'u_j'\, e_j E_x' = \sum_{k \neq j} (\varepsilon_{jk} + u_j' P_{jk}) \quad , \tag{2.6}$$

where κ is the thermal conductivity, T the absolute temperature and ξ_{jk} denotes the kinetic energy transfer from the k-particles to the j-particles. The basic system is completed by the equations of state for the three species

$$p_j' = n_j' \, kT_j' \quad . \tag{2.7}$$

With the dissipative coefficients and transfer terms assumed to be known functions of the dependent variables, then Eqs. (2.1) to (2.7) constitute a system of thirteen equations for the thirteen unknowns u_j', n_j', T_j', p_j' and E_x'. However, since the continuity and state equations are algebraic, and six in number, the problem is reducible to the solution of seven simultaneous differential equations for the appropriate seven unknowns.

We may simplify the system of equations first by noting that from Newton's third law of motion,

$$P_{jk} + P_{kj} \equiv 0 \quad , \tag{2.8}$$

$$\xi_{jk} + u'_j P_{jk} + \xi_{kj} + u'_k P_{kj} \equiv 0 \quad . \tag{2.9}$$

Secondly, we note that the electron inertia and viscous terms are much smaller than the corresponding ion and atom terms and may therefore be neglected.

After employing the above conditions and approximations the basic set of shock structure equations will consist of the two algebraic continuity equations (2.2) and (2.3), Poisson's equation (2.1), and the following six differential equations:

a. The electron momentum equation (2.5), j = e

$$\frac{d}{dx'}(n_e' kT_e') + n_e' e E_x' = P_{ei} + P_{ea} \quad . \tag{2.10}$$

b. The ion-electron momentum equation, obtained by adding the ion and electron momentum equations

$$m_i C_i \frac{du_i'}{dx'} + \frac{d}{dx'}(n_i' kT_i' + n_e' kT_e') - \frac{d}{dx'}\left(\mu_i'' \frac{du_i'}{dx'}\right)$$

$$- (n_i' - n_e') eE_x' = P_{ia} + P_{ea} \quad . \tag{2.11}$$

c. The plasma momentum equation, obtained by adding the momentum equations for the three species. On using Eqs. (2.1) and (2.8), the resulting equation can be integrated once to give

$$m_i(C_a u_a' + C_i u_i') + n_a' kT_a' + n_i' kT_i' + n_e' kT_e'$$

$$- \mu_a'' \frac{du_a'}{dx'} - \mu_i'' \frac{du_i'}{dx'} - \frac{E_x'^2}{8\pi} = P \quad . \tag{2.12}$$

Here the atom mass is assumed to be equal to the ion mass and the constant of integration P is determined by the boundary conditions.

d. The electron internal energy equation, which is obtained by multiplying the electron momentum equation by u'_e and subtracting the result from the electron energy equation. It may be written

$$\frac{3}{2} C_i k \frac{dT'_e}{dx'} + C_i \frac{kT'_e}{u'_e} \frac{du'_e}{dx'} - \frac{d}{dx'} \left(\kappa_e \frac{dT'_e}{dx'}\right) = \xi_{ea} + \xi_{ei} \quad . \tag{2.13}$$

e. The ion internal energy equation, obtained by the same process as Eq. (2.13), which may be written

$$\frac{3}{2} C_i k \frac{dT'_i}{dx'} + C_i \frac{kT'_i}{u'_i} \frac{du'_i}{dx'} - u''_i \left(\frac{du'_i}{dx'}\right)^2 - \frac{d}{dx'} \left(\kappa_i \frac{dT'_i}{dx'}\right)$$

$$= \xi_{ia} + \xi_{ie} \quad . \tag{2.14}$$

f. The plasma energy equation, obtained by adding Eqs. (2.6) for the three species with the aid of Eq. (2.9) and integrating the resulting equation to give

$$m_i \frac{C_a}{2} u'^2_a + m_i \frac{C_i}{2} u'^2_i + \frac{5}{2} k[C_a T'_a + C_i(T'_i + T'_e)] - \kappa_a \frac{dT'_a}{dx'}$$

$$- \kappa_i \frac{dT'_i}{dx'} - \kappa_e \frac{dT'_e}{dx'} - u'_a \mu''_a \frac{du'_a}{dx'} - u'_i \mu''_i \frac{du'_i}{dx'} = H \quad , \tag{2.15}$$

where the constant of integration H is evaluated at the boundary conditions.

III. DISSIPATION AND TRANSFER COEFFICIENTS

We now evaluate the dissipation and transfer coefficients which are present in the shock structure equations (2.1) - (2.15). The classical coefficients of viscosity and thermal conduction for a pure monatomic gas are given respectively by the relations[7]

$$\mu = \frac{5\pi}{32} n' m c \left(\frac{c}{\nu}\right) \quad , \tag{3.1}$$

$$\kappa = \frac{15k}{4m} \mu = \frac{75}{128} \pi k n' \left(\frac{c}{\nu}\right) \quad , \tag{3.2}$$

where $c = (8\ kT'/\pi m)^{1/2}$ is the mean thermal speed, ν the collision frequency and k the Boltzmann constant. The collision frequency for a pure gas is equal to:

$$\nu = \sqrt{2}\ n' Q'_{aa} c \quad , \tag{3.3}$$

where Q'_{aa} is the effective hard sphere cross section for atom-atom collisions.

The relations (3.1) and (3.2) can be extended to the component ℓ of a gas mixture as follows[8]:

---

7. S. Chapman and T. G. Cowling The Mathematical Theory of Non-Uniform Gases, (Cambridge University Press, New York, 1952) pp. 100-104.

8. J. A. Fay, "Hypersonic Heat Transfer in the Air Laminar Boundary Layer," Avco Everett Research Lab. AMP 71, March 1962.

$$\mu_\ell = \frac{5\pi}{32} n'_\ell m_\ell c_\ell \left(\frac{c_\ell}{\nu_\ell}\right) \quad , \tag{3.4a}$$

$$\kappa_\ell = \frac{15k}{4m_\ell} \mu_\ell \quad , \tag{3.4b}$$

where ν_ℓ is the total collision frequency for momentum exchange given by

$$\nu_\ell = \sum_k n'_k Q'_{\ell k} (c_\ell^2 + c_k^2)^{1/2} \frac{2m_{\ell k}}{m_\ell} \quad . \tag{3.5}$$

Here, k is summed over all components of the mixture, $m_{\ell k} = m_\ell m_k/(m_\ell + m_k)$ is the reduced mass, $(c_\ell^2 + c_k^2)^{1/2}$ is the mean relative thermal velocity and $2m_{\ell k}/m_\ell$ is the fraction of momentum transferred per collision between 2 particles of arbitrary mass. The quantity $Q'_{\ell k}$ is the collision cross section for particles ℓ and k. For a pure gas, ν_ℓ reduces to ν defined by Eq. (3.3).

On developing the relation (3.5), the atom, ion, and electron collision frequencies may be written respectively as

$$\nu_a = n'_a Q'_{aa} \left(16 \frac{kT'_a}{\pi m_i}\right)^{1/2} + n'_i Q'_{ia} \left[8k\left(\frac{T'_a + T'_i}{\pi m_i}\right)\right]^{1/2} + n'_e Q'_{ea} \left(\frac{8kT'_e}{\pi m_e}\right)^{1/2} \frac{2m_e}{m_i} \quad , \tag{3.6}$$

$$\nu_i = n'_a Q'_{ia} \left[8k\left(\frac{T'_a + T'_i}{\pi m_i}\right)\right]^{1/2} + n'_i Q'_{ii} \left(16 \frac{kT'_i}{\pi m_i}\right)^{1/2} + n'_e Q'_{ei} \left(8 \frac{kT'_e}{\pi m_e}\right)^{1/2} \frac{2m_e}{m_i} \quad , \tag{3.7}$$

$$\nu_e = 2n'_a Q'_{ea}\left(8\frac{kT'_e}{\pi m_e}\right)^{1/2} + 2n'_i Q'_{ei}\left(8\frac{kT'_e}{\pi m_e}\right)^{1/2} + n'_e Q'_{ee}\left(16\frac{kT'_e}{\pi m_e}\right)^{1/2} \quad . \tag{3.8}$$

The last terms of Eqs. (3.6) and (3.7) represent the effect of the electron-heavy particle collisions and are of the order of ε^2 where

$$\varepsilon = \left(\frac{m_e}{m_i}\right)^{1/2} = \frac{1}{275} \qquad \text{for Argon.}$$

These terms are very small and will be neglected in comparison to one. It is now necessary to evaluate the various cross sections remaining in the above relations.

The cross sections for collisions between electrically charged particles are deduced from the value of the viscosity coefficient for an ionized gas given by Chapman and Cowling[9]. Using the Spitzer[10] result that the Debye length is the proper cutoff impact parameter, one finds

$$\mu = \frac{5}{8}\left(\frac{m}{\pi}\right)^{1/2}\frac{(kT')^{5/2}}{e^4 \log_e \Lambda} \quad , \tag{3.9}$$

where Λ is a dimensionless cutoff impact parameter equal to $3(k^3T'^3/\pi n')^{1/2}/2e^3$. Comparing Eqs. (3.1) and (3.9) we obtain the following values for the Coulomb cross section:

$$Q'_{jj} = \frac{\pi e^4 \log_e \Lambda}{2(kT'_j)^2} \quad , \quad j = i, e \quad . \tag{3.10}$$

---

9. See Ref. 7, p. 179.

10. L. Spitzer Jr., Physics of Fully Ionized Gases (Interscience Publishers, Inc., New York, 1956) p. 72.

Since $T'_e/m_e \gg T'_i/m_i$ the electron temperature is the relevant temperature in the calculation of ion-electron collision cross section and

$$Q'_{ei} = Q'_{ee} \quad . \tag{3.11}$$

The values of the other required cross sections Q'_{aa}, Q'_{ia}, and Q'_{ea} depend on the gas considered. They will here be evaluated from experimental results for Argon. The atom-atom collision cross section Q'_{aa} is obtained from the values of the viscosity coefficient μ_a given by Amdur and Mason[11]. At high temperatures $\mu_a \simeq 31.10^{-7}\ T'^{3/4}_a$ g/cm sec, which corresponds to

$$Q'_{aa} = 170.10^{-16}/T'^{1/4}_a \ \text{cm}^2 \quad .$$

Experimental data compiled by Fay[8] show that the atom-ion cross section Q'_{ia} is much bigger than the atom-atom cross section because of the charge exchange mechanism. This cross section decreases very slowly with the temperature and will be taken constant and given by

$$Q'_{ia} = 140 \cdot 10^{-16} \ \text{cm}^2 \quad .$$

---

11. I. Amdur and E. A. Mason, Phys. Fluids 1, 370, (1958).

The atom-electron cross section Q'_{ea} [12,13] has a low minimum of $0.25 \cdot 10^{-16}$ cm^2 at $T'_e = 4600^oK$ because of the strong Ramsauer effect. It increases rapidly for higher temperatures up to 10^6 ^oK and decreases again. For a range of temperature up to $5 \cdot 10^5$ ^oK we shall use the following approximate relations obtained from Ref. 12 by curve fitting

$$Q'_{ea} = (-0.35 + 0.775\ 10^{-4}\ T'_e) \times 10^{-16}\ \text{cm}^2 \qquad T'_e > 10^4\ ^oK$$

$$Q'_{ea} = (0.39 - 0.551\ 10^{-4}\ T'_e + 0.595\ 10^{-8}\ T'^2_e) \cdot 10^{-16}\ \text{cm}^2 \qquad T'_e < 10$$

In any case the momentum and energy exchange between electrons and atoms is so slow that the structure of the shock itself depends only very weakly on the cross section Q'_{ea}.

For generality the analysis will be carried out with the cross sections expressed as known functions of the temperature which are not explicitly specified. The results obtained will be qualitatively valid for other values of the cross sections provided that the essential feature $Q'_{ia} >> Q'_{aa}$ is retained.

The viscosity and thermal conduction coefficients for the atom gas may then be written in the form

$$\mu_a = \frac{5}{16 Q'_{aa}} \frac{(m_i\ kT'_a)^{1/2}}{\left[1 + \frac{n'_i\ Q'_{ia}}{n'_a\ Q'_{aa}} \left(\frac{T'_a + T'_i}{2T'_a}\right)^{1/2}\right]} \quad , \qquad (3.12a)$$

---

12. I. P. Shkarofsky, M. P. Bachynski and T. W. Johnston, Planetary and Space Science 6, 24, 1961

13. S. C. Brown, Basic Data of Plasma Physics (The Technology Press of the Massachusetts Institute of Technology, and J. Wiley and Sons Inc., N. Y., 1959) p. 19.

$$\kappa_a = \frac{\frac{75k}{64Q'_{aa}} \left(\frac{\pi k T'_a}{m_i}\right)^{1/2}}{\left[1 + \frac{n'_i Q'_{ia}}{n'_a Q'_{aa}} \left(\frac{T'_a + T'_i}{2T'_a}\right)^{1/2}\right]} \quad . \tag{3.12b}$$

by

We note that the viscosity and thermal conduction coefficients of the atom gas are reduced by the presence of the ions.

For the ion gas these coefficients are given by

$< 10^4\ ^oK$

$$\mu_i = \frac{\frac{5n'_i}{16Q'_{ia}n'_a} (\pi m_i k)^{1/2}\ T'_i}{\left(\frac{T'_a + T'_i}{2}\right)^{1/2} \left[1 + \frac{n'_i Q'_{ii}}{n'_a Q'_{ia}} \left(\frac{2T'_i}{T'_a + T'_i}\right)^{1/2}\right]} \quad , \tag{3.13a}$$

$$\kappa_i = \frac{\frac{75n'_i}{64Q'_{ia}n'_a} \left(\frac{\pi k}{m_i}\right)^{1/2}\ k T'_i}{\left(\frac{T'_a + T'_i}{2}\right)^{1/2} \left[1 + \frac{n'_i Q'_{ii}}{n'_a Q'_{ia}} \left(\frac{2T'_i}{T'_a + T'_i}\right)^{1/2}\right]} \quad , \tag{3.13b}$$

while for the electron gas

$$\kappa_e = \frac{75\left(\frac{\pi k T'_e}{m_e}\right)^{1/2}\ k}{64Q'_{ee}(1 + \sqrt{2})\ \left(1 + \frac{\sqrt{2}\ n'_a Q'_{ea}}{(1 + \sqrt{2})\ n'_e Q'_{ee}}\right)} \tag{3.14}$$

The viscosity and thermal conduction coefficients of the ionized particles are here reduced by the presence of atoms. The electron viscosity coefficient is smaller than μ_i by a factor of the order of $\varepsilon = (\frac{m_e}{m_i})^{1/2}$ and the electron viscosity term may be neglected in the structure equations, as it was noted earlier.

From Eqs. (2.12) and (2.15), we note that for given values of the Mach number, velocities and temperatures, the velocity and temperature gradients are inversely proportional to the viscosity and the thermal conduction coefficients. Since, from Eq. (2.10) the electric field is proportional to a temperature and velocity gradient, the whole shock structure depends critically on the behavior of the dissipation coefficients. As the viscosity and thermal conduction of the atoms coefficients are progressively replaced by those of the ions as the main dissipative mechanisms, the plasma regime changes from weakly ionized to fully ionized and the shock structure varies accordingly. The different plasma regimes for Argon are illustrated in the α, T' diagram of Fig. 1. When $n_i'Q_{ii}' << n_a'Q_{ia}'$ and $n_i'Q_{ia}' << n_a'Q_{aa}'$, it may be seen from Eqs. (3.12) and (3.13) that the ion and atom dissipative coefficients depend mostly on the atoms. Moreover, if $\alpha << 1$ the ion dissipation is negligible compared with the atom dissipation and the region delimited by the three preceding inequalities represents the weakly ionized regime. On the other hand, when $n_i'Q_{ia}' >> n_a'Q_{aa}'$ and $n_i'Q_{ii}' >> n_a'Q_{ia}'$, the atom collisional dissipation is much smaller than the ion dissipation and the ion viscosity and thermal conduction approach

their fully ionized value: this we term the quasi-fully ionized region. Finally, the intermediate range between $\alpha = 10^{-3}$ and $\alpha = 0.5$ represents a mixed regime that we denote by partially ionized.

The momentum exchanges between the different species of a partially ionized gas have been computed by Zhdanov[14]. On neglecting thermal diffusion but extending Zhdanov's results to a multi-temperature model, the momentum transfer per unit volume from species k to species j is given by

$$P_{jk} = - n'_j m_{jk} Z_{jk}^{-1}(u'_j - u'_k) \quad , \tag{3.15}$$

where

$$Z_{jk}^{-1} = \frac{4}{3} n'_k \left(\frac{8kT'_j}{\pi m_j} + \frac{8kT'_k}{\pi m_k}\right)^{1/2} Q'_{jk} \quad . \tag{3.16}$$

The quantity Z_{jk} is of the same order as the collision time. In particular, the ion-atom momentum transfer is

$$P_{ai} = - \frac{4}{3} \sqrt{2}\, n'_a n'_i \left[\frac{m_i}{\pi} k(T'_a + T'_i)\right]^{1/2} Q'_{ia}(u'_a - u'_i) \quad . \tag{3.17}$$

Using the inequality $\frac{T'_e}{m_e} >> \frac{T'_i}{m_i}$ the electron-atom momentum transfer is,

$$P_{ae} = - \frac{8}{3} \sqrt{2}\, n'_a u'_e \left(\frac{m_e kT'_e}{\pi}\right)^{1/2} Q'_{\epsilon a}(u'_a - u'_e) \tag{3.18}$$

---

14. Zhdanov V. M., PMM 26, 280, (1962). [Eng. Transl.: Applied Mathematics and Mechanics 26, 401 (1962).]

Since

$$m_i^{1/2} >> m_e^{1/2}$$

it follows that

$$P_{ai} >> P_{ae}$$

The ion-electron momentum transfer is given by

$$P_{ei} = -\frac{8}{3}\sqrt{2}\, n_i' n_e' \left(\frac{m_e\, kT_e'}{\pi}\right)^{1/2} Q_{ei}'(u_e' - u_i') \quad . \qquad (3.19)$$

The total ion-electron energy transfer has been computed by Burgers[15]. Expanding Burgers' result in powers of the small quantity $\varepsilon = \left(\frac{m_e}{m_i}\right)^{1/2}$ we find that the ion-electron energy transfer may be written[1]

$$\xi_{ei} + u_e' P_{ei} = -8\sqrt{2}\, n_i' n_e' \left(\frac{m_e\, kT_e'}{\pi}\right)^{1/2} \frac{Q_{ei}'}{m_i}\left[k(T_e' - T_i')\right.$$

$$\left. + \frac{1}{3}(u_e' - u_i')\,(m_i u_i' + m_e u_e')\right] \quad . \qquad (3.20)$$

Petschek and Byron[16] have computed the atom-electron energy transfer due to the random motion of the particles for arbitrary interaction laws which is given by

---

15. J. M. Burgers, in Plasma Dynamics, edited by F. H. Clauser (Addison-Wesley Publishing Co., Reading, Mass., 1960) p. 156.

16. H. Petschek and S. Byron, Annals of Physics 1, 270, (1957).

$$\Delta E = - \frac{m_e^2}{m_i} \frac{(T'_a - T'_e)}{T'_e} n'_a n'_e \int c_e^3 \, \sigma(c_e) \, f_e \, d\vec{c}_e \quad , \qquad (3.21)$$

where $\vec{c}_e$ is the random electron velocity, $\sigma(c_e)$ the cross section and f_e the Maxwell distribution function. The integral term in Eq. (3.21) represents the mean value of the product $c_e^3 \, \sigma(c_e)$. Recalling that Q'_{ea} is the cross section averaged over a Maxwell distribution and approximating the mean value of the product $c_e^3 \, \sigma(c_e)$ by the product of the averages of the two terms, we obtain

$$\Delta E \approx - 8 \sqrt{2} \, n'_a n'_e \left(\frac{m_e \, kT'_e}{\pi}\right)^{1/2} \frac{Q'_{ea}}{m_i} k(T'_a - T'_e) \qquad (3.22)$$

The total energy transfer is the sum of the energy transfers due to the random and directed motions of the particles and is given by

$$\xi_{ae} + u'_a P_{ae} = - 8 \sqrt{2} \, n'_a n'_e \left(\frac{m_e \, kT'_e}{\pi}\right)^{1/2} \frac{Q'_{ea}}{m_i} \left[k(T'_a - T'_e) + \frac{(u'_a - u'_e)}{3} (m_i u'_a + m_e u'_e)\right] \quad . \qquad (3.23)$$

The ion-atom energy transfer is derived in Appendix A and the result is

$$\xi_{ai} + u'_a P_{ei} = - 2 \sqrt{2} \, n'_a n'_i \left[\frac{k}{\pi m_i} (T'_a + T'_i)\right]^{1/2} Q'_{ia} \left[k(T'_a - T'_i) + \frac{m_i}{3} (u'_a - u'_i) (u'_a + u'_i)\right] \quad . \qquad (3.24)$$

IV. DIMENSIONLESS EQUATIONS AND BOUNDARY CONDITIONS

At upstream infinity ($x' \to -\infty$) and at downstream infinity ($x' \to +\infty$) all gradients vanish and the system of equations (2.1) - (2.15) reduces to the Hugoniot conditions. We note that on each side of the shock, the three species have the same velocity and temperature, and the electric field vanishes.

Since the shock thickness depends generally on the downstream state, we choose to normalize the velocities and temperatures with respect to their downstream values after the shock. In what follows we denote the upstream state by subscript 1 and the downstream state by subscript 2. On this basis we set

$$u_j = u_j'/u_2' \quad , \quad T_j = T_j'/T_2' \quad , \tag{4.1}$$

with $j = i$, e, and a. We note that the dimensionless velocities are of order of one but the upstream dimensionless temperatures are very small for strong shocks.

The appropriate dimensionless electric field is

$$E = \frac{eE_x' \lambda_{D_2}}{kT_2'} \quad , \tag{4.2}$$

where $\lambda_{D_2} = \left(\frac{kT_2'}{4\pi e^2 n_{e_2}'}\right)^{1/2}$ is the downstream Debye length. The corresponding dimensionless potential ϕ is

$$\phi = \frac{e\phi'}{kT_2'} \quad , \tag{4.3}$$

where ϕ' is the actual potential.

We also introduce the dimensionless charge separation defined by the relation

$$\delta = \frac{n_i' - n_e'}{n_{i_2}'} = \frac{1}{u_i} - \frac{1}{u_e} \quad . \tag{4.4}$$

The independent variable is made dimensionless with respect to the shock thickness Δ_s by the relation

$$x_s = x'/\Delta_s \quad , \tag{4.5}$$

The cross sections $Q'_{\alpha\beta}$ are normalized with respect to their downstream values by the relation

$$Q_{\alpha\beta} = Q'_{\alpha\beta}/Q'_{\alpha\beta_2} \tag{4.6}$$

It is convenient at this point to introduce the following mean free paths which are related to the various downstream cross-section $Q'_{\alpha\beta_2}$:

atom-atom mean free path

$$\ell_{aa_2} = (\sqrt{2}\, n'_{a_2}\, Q'_{aa_2})^{-1} \quad , \tag{4.7a}$$

ion-ion mean free path

$$\ell_{ii_2} = (\sqrt{2}\, n'_{i_2}\, Q'_{ii_2})^{-1} \quad , \tag{4.7b}$$

atom-ion mean free path

$$\ell_{ia_2} = (\sqrt{2}\, n'_{a_2}\, Q'_{ia_2})^{-1} \quad , \tag{4.7c}$$

atom-electron mean free path

$$\ell_{ea_2} = (\sqrt{2}\, n'_{a_2}\, Q'_{ea_2})^{-1} \quad . \tag{4.7d}$$

Since $n'_{i_2} = n'_{e_2}$, $Q'_{ee_2} = Q'_{ei_2} = Q'_{ii_2}$, the ion-electron and the electron-electron mean free paths are both equal to the ion-ion mean free path.

Finally, we define the downstream plasma Mach number M_2 by the relation

$$M_2^2 = \frac{u_2'^2}{\dfrac{5(2n'_{i_2} + n'_{a_2})\, kT'_2}{3m_i(n'_{a_2} + n'_{i_2}) + m_e n'_{i_2}}} \approx \frac{m_i u_2'^2}{\frac{5}{3}\, kT'_2\, (1 + \alpha)} \quad , \tag{4.8}$$

where as previously the electron mass is neglected in comparison to the ion mass.

If we employ the non-dimensionalization of Eqs. (4.1) - (4.8) neglecting terms of order ε and smaller, such as the electron viscosity and inertia terms, then we may write in dimensionless form:

Poisson's equation (from Eq. (2.1))

$$\frac{dE}{dx_s} = \frac{\Delta_s}{\lambda_{D_2}}\, \delta \quad . \tag{4.9}$$

On the other hand, the electron momentum equation is given from Eq. (2.5) with j = e by

$$\frac{d}{dx_s}\left(\frac{T_e}{u_e}\right) + \frac{\Delta_s E}{\lambda_{D_2} u_e} = -\alpha\varepsilon\Delta_s T_e^{1/2}\left[\frac{Q_{ae}}{\ell_{ae_2}}\left(\frac{1}{u_a} - \frac{1}{u_e}\right) + \frac{Q_{ei}}{\ell_{ii_2}}\delta\right] .$$

From the above relation we see that

$$E = O\left(\frac{\lambda_{D_2}}{\Delta_s}\right) ,$$

while from Eq. (4.9)

$$\delta = O\left(\frac{\lambda_{D_2}}{\Delta_s} E\right) = O\left(\frac{\lambda_{D_2}^2}{\Delta_s^2}\right) .$$

In most plasmas, the Debye length is much smaller than the mean free path, and therefore much smaller than the shock thickness. It follows that the dimensionless quantities E and δ are very small and can be neglected in comparison to one. Therefore, in all structure equations, except Poisson's equation (4.9) we set

$$\delta = 0 ,$$

$$u_e = u_i ,$$

$$E = O\left(\frac{\lambda_{D_2}}{\Delta_s}\right) \approx 0 .$$

We note that the ion and electron fluids move together although their temperatures may be different.

With the approximations noted above our basic dimensionless equations in addition to Poisson's equation may be written:

Electron momentum equation (from Eq. (2.5))

$$\frac{d}{dx_s}\left(\frac{T_e}{u_i}\right) + \frac{\Delta_s E}{\lambda_{D_2} u_i} = -a\varepsilon \frac{\Delta_s}{\ell_{ea_2}} T_e^{1/2} Q_{ea}\left(\frac{1}{u_a} - \frac{1}{u_i}\right) . \quad (4.10)$$

Ion-electron momentum equation (from Eq. (2.11))

$$\frac{5}{3} M_2^2(1+\alpha)\frac{du_i}{dx_s} + \frac{d}{dx_s}\left(\frac{T_i + T_e}{u_i}\right) - c\frac{\ell_{ia_2}}{\Delta_s}\frac{d}{dx_s}\left(\frac{T_i^{1/2}}{F_i}\frac{du_i}{dx_s}\right)$$

$$= -\frac{a}{2}\Delta_s\left(\frac{1}{u_a} - \frac{1}{u_i}\right)\left[\frac{Q_{ia}}{\ell_{ia_2}}(T_a + T_i)^{1/2} + 2\varepsilon\frac{Q_{ea}}{\ell_{ea_2}} T_e^{1/2}\right] . \quad (4.11)$$

Plasma momentum equation (from Eq. (2.12))

$$\frac{5}{3} M_2^2(1+\alpha)\left[u_a - 1 + \frac{\alpha}{1-\alpha}(u_i - 1)\right] + \frac{T_a}{u_a} - 1 + \frac{\alpha}{1-\alpha}\left(\frac{T_i + T_e}{u_i} -\right.$$

$$-c\frac{\ell_{aa_2}}{\Delta_s}\frac{T_a^{1/2}}{F_a}\frac{du_a}{dx_s} - c\frac{\alpha}{1-\alpha}\frac{\ell_{ia_2}}{\Delta_s}\frac{T_i^{1/2}}{F_i}\frac{du_i}{dx_s} = 0 . \quad (4.12)$$

Electron internal energy equation (from Eq. (2.13))

$$\frac{3}{2}\frac{dT_e}{dx_s} + \frac{T_e}{u_i}\frac{du_i}{dx_s} - f\frac{\ell_{ii_2}}{\epsilon\Delta_s}\frac{d}{dx_s}\left(\frac{T_e^{1/2}}{F_e}\frac{dT_e}{dx_s}\right) = -b\epsilon\frac{\Delta_s}{\ell_{ea_2}}\frac{T_e^{1/2}}{u_a u_i}Q_{ea}$$

$$\left[T_e - T_a - \frac{5}{9}M_2^2(1+\alpha)(u_i - u_a)^2\right] - \frac{b\epsilon\Delta_s T_e^{1/2}}{\ell_{ii_2}u_i^2}Q_{ee}(T_e - T_i) \quad . \tag{4.13}$$

Ion internal energy equation (from Eq. (2.14))

$$\frac{3}{2}\frac{dT_i}{dx_s} + \frac{T_i}{u_i}\frac{du_i}{dx_s} - c\frac{\ell_{ia_2}}{\Delta_s}\frac{T_i^{1/2}}{F_i}\left(\frac{du_i}{dx_s}\right)^2 - d\frac{\ell_{ia_2}}{\Delta_s}\frac{d}{dx_s}\left(\frac{T_i^{1/2}}{F_i}\frac{dT_i}{dx_s}\right)$$

$$= -\frac{b\Delta_s}{4\ell_{ia_2}}Q_{ia}\frac{(T_a + T_i)^{1/2}}{u_a u_i}\left[T_i - T_a + \frac{5}{9}M_2^2(1+\alpha)\,u_a(u_i - u_a)\right]$$

$$-\frac{b\epsilon\Delta_s}{\ell_{ii_2}}\frac{T_e^{1/2}}{u_i^2}(T_i - T_e)\,Q_{ee} \quad . \tag{4.14}$$

Plasma energy equation (from Eq. (2.15))

$$\frac{T_e}{} - 2)$$

$$\frac{5}{6}M_2^2(1+\alpha)\left[u_a^2 - 1 + \frac{\alpha}{1-\alpha}(u_i^2 - 1)\right] + \frac{5}{2}\left[T_a - 1 + \frac{\alpha}{1-\alpha}(T_i + T_e - 2)\right]$$

$$-d\frac{\ell_{aa_2}}{\Delta_s}\frac{T_a^{1/2}}{F_a}\frac{dT_a}{dx_s} - c\frac{\ell_{aa_2}}{\Delta_s}\frac{u_a T_a^{1/2}}{F_a}\frac{du_a}{dx_s} - f\frac{\alpha}{(1-\alpha)}\frac{\ell_{ii_2}}{\epsilon\Delta_s}\frac{T_e^{1/2}}{F_e}\frac{dT_e}{dx_s}$$

$$-\frac{\alpha T_i^{1/2}\ell_{ia_2}}{(1-\alpha)F_i\Delta_s}\left(d\frac{dT_i}{dx_s} + cu_i\frac{du_i}{dx_s}\right) = 0 \quad . \tag{4.15}$$

The dimensionless potential may be obtained from the relation

$$\phi = -\frac{e}{kT_2'}\int E_x' dx' = -\int \frac{\Delta_s}{\lambda_{D_2}} E \, dx_s \quad . \tag{4.16}$$

The quantities, a, b, c, d, f, F_a, F_i, and F_e appearing in the dimensionless equations (4.10) - (4.15) are defined as follows:

$$a = \frac{8}{3}\left(\frac{5(1+\alpha)}{3\pi}\right)^{1/2} M_2 \quad , \quad b = \frac{8}{\left(\frac{5\pi(1+\alpha)}{3}\right)^{1/2} M_2} \, ,$$

$$c = \frac{5}{12}\left(\frac{10\pi(1+\alpha)}{3}\right)^{1/2} M_2 \quad , \quad d = \frac{75}{64 M_2}\left(\frac{6\pi}{5(1+\alpha)}\right)^{1/2} \, ,$$

$$f = \frac{d}{1+\sqrt{2}} \quad . \tag{4.17}$$

$$F_a = Q_{aa} + \frac{\alpha \ell_{aa_2}}{(1-\alpha)\,\ell_{ia_2}} Q_{ia} \frac{u_a}{u_i}\left(\frac{T_a + T_i}{2T_a}\right)^{1/2} \quad , \tag{4.18}$$

$$F_i = Q_{ii}\frac{\ell_{ia_2}}{\ell_{ii_2}} + \frac{u_i}{u_a}\left(\frac{T_a + T_i}{2T_i}\right)^{1/2} Q_{ia} \tag{4.19}$$

$$F_e = Q_{ee} + \frac{\sqrt{2}\,\ell_{ii_2}\, Q_{ea} u_i}{(1+\sqrt{2})\,\ell_{ea_2}\, u_a} \tag{4.20}$$

When the quantities F_a, F_i, and F_e are replaced by the definitions given above, Eqs. (4.9) - (4.15) represent a set of

seven equations for the seven unknown variables u_a, u_i, T_a, T_i, T_e, E and δ as a function of the independent variable x_s. Had we normalized the variables with respect to their upstream values we would have received precisely the same set of equations with the subscript 1 replacing the subscript 2 in the parameters.

Any state of the plasma will be represented by a point in the seven dimensional phase space whose coordinates are the dependent variables. The states 1 and 2 upstream and downstream of the shock respectively, are singular points of the system of Eqs. (4.9) - (4.15). The dimensionless Hugoniot relations obtained by setting the derivatives equal to zero specify the coordinates of these singular points. In particular the coordinates of point 1 are

$$E_1 = 0$$

$$u_{a_1} = u_{i_1} = u_1 = \frac{M_2^2 + 3}{4M_2^2} \quad ,$$

$$T_{a_1} = T_{i_1} = T_1 = \frac{(5M_2^2 - 1)(M_2^2 + 3)}{16M_2^2} \quad , \qquad (4.21)$$

while the coordinates of point 2 are

$$E_2 = 0 \quad ,$$

$$u_{a_2} = u_{i_2} = u_2 = 1$$

$$T_{a_2} = T_{i_2} = T_2 = 1 \quad . \qquad (4.22)$$

Here the Mach number behind the shock M_2 is related to the free stream Mach number M_1 by the relation

$$M_2^2 = \frac{M_1^2 + 3}{5M_1^2 - 1} \quad . \tag{4.23}$$

It is important to note that the Hugoniot conditions depend on the plasma Mach number only. For the same velocity and temperature conditions upstream, the plasma Mach number and therefore the shock strength are reduced when the degree of ionization increases.

A shock will exist whenever $u_1 > 1$, which requires $M_1 > 1$. The atom and ion Mach numbers are greater than the plasma Mach number by the factor $(1 + \alpha)^{1/2}$, and the atom and ion flows are supersonic when $M_1 > 1$. The electron Mach number is proportional to ϵ times the plasma Mach number, so that the electron flow is subsonic unless M_1 is very large.

The shock thicknesses Δ_s in which the various collisional effects are important can now be estimated from the appropriate terms in the dimensionless equations. For example, we note from Eq. (4.13) that the electron thermal conduction term is of the order of $\ell_{ii_2}/\epsilon\Delta_s$; it is therefore of order one when Δ_s is $O(\ell_{ii_2}/\epsilon)$. This implies that the electron thermal conduction can broaden the shock to a thickness of the order of ℓ_{ii_2}/ϵ. In the weakly and partially ionized regimes where the dimensionless expressions F_a, F_i, and F_e are $O(1)$, the possible shock thicknesses and their corresponding collisional mechanisms are:

Mechanisms	Shock thickness
Electron thermal conduction,	ℓ_{ii_2}/ε
electron-ion energy transfer,	ℓ_{ii_2}/ε
electron-atom energy and momentum transfer,	ℓ_{ea_2}/ε
atom thermal conduction and viscosity,	ℓ_{aa_2}
ion thermal conduction and viscosity,	ℓ_{ia_2}
atom-ion momentum and energy transfer,	ℓ_{ia_2}

Obviously the shock structure will depend on the relative magnitude of the various mean free paths. The values of the ratios ℓ_{ia_2}/ℓ_{aa_2}, ℓ_{ea_2}/ℓ_{ii_2} and ℓ_{ia_2}/ℓ_{ii_2} are plotted in Fig. 2 as a function of the temperature for different values of the degree of ionization for Argon. It may be noted that the ratio ℓ_{ia_2}/ℓ_{aa_2} is independent of α and is always small compared to one. The ion-ion mean free path ℓ_{ii_2} is larger than the atom-atom mean free path ℓ_{aa_2} for low degrees of ionization but it is smaller than ℓ_{aa_2} for $\alpha = 0.5$ and $T' < 2.5\ 10^5\ ^oK$.

In the quasi-fully ionized regime $F_a = O(\ell_{aa_2}/\ell_{ia_2})$, $F_i = O(\ell_{ia_2}/\ell_{ii_2})$ and the atom thermal conductivity and viscosity lead to a shock thickness $O(\ell_{ia_2})$ while the ion thermal conduction and viscosity correspond to a shock thickness $O(\ell_{ii_2})$. The shock thicknesses corresponding to the other collisional mechanisms are not modified. However we shall not consider this regime because of its similarity with the fully ionized case[1].

V. WEAKLY IONIZED PLASMA $\alpha << 1$

We consider first the case of the weakly ionized plasma, because of the simplifications introduced by the assumption $\alpha << 1$. The atom gas is indeed unaffected by the charged particles provided that the degree of ionization is very small. We note that the terms representing the charged particles in Eqs. (4.12) and (4.15) are proportional to α and can be neglected when $\alpha << 1$. Moreover, when α is so small that $\alpha \ell_{aa_2} / \ell_{ia_2} << 1$, for example when $\alpha = 10^{-3}$, Eq. (4.18) yields

$$F_a \tilde{\sim} Q_{aa} \tag{5.1}$$

With the approximations described above, Eqs. (4.12) and (4.15) govern the atom velocity and temperature distributions in the atom shock and are completely uncoupled from the other variables.

We first examine the thermal layer of thickness ℓ_{ii_2}/ε. Should a discontinuous solution arise within this layer, we introduce at the discontinuity a shock layer whose thickness is the next smaller length until a continuous transition is found from the upstream state to the downstream one.

When $\Delta_s = \ell_{ii_2}/\varepsilon$, x_s is replaced by $x^* = \varepsilon x'/\ell_{ii_2}$. On neglecting terms of order of α and ε in Eqs. (4.9) - (4.16), we obtain a simplified system of shock layer equations. From Eqs. (4.12) and (4.15)

$$\frac{5}{3} M_2^2(u_a - 1) + \frac{T_a}{u_a} - 1 = 0 \quad , \tag{5.2}$$

$$\frac{5}{6} M_2^2(u_a^2 - 1) + \frac{5}{2}(T_a - 1) = 0 \quad . \tag{5.3}$$

Equations (5.2) and (5.3) are identical to the Hugoniot conditions and yield the following discontinuous solution:

$$\text{near point 1} \quad u_a = u_1 \quad , \quad T_a = T_1 \quad , \tag{5.4}$$

$$\text{near point 2} \quad u_a = u_2 = 1 \quad , \quad T_a = T_2 = 1 \quad . \tag{5.5}$$

This discontinuous solution indicates that there is a thinner atom shock imbedded within the layer of thickness ℓ_{ii_2}/ε and this shock will be studied later. Outside the shock the atom flow is uniform.

From Eqs. (4.11) and (4.14) we find

$$u_i = u_a + O(\varepsilon \ell_{ia_2}/\ell_{ii_2}) \quad , \tag{5.6}$$

$$T_i = T_a + O(\varepsilon \ell_{ia_2}/\ell_{ii_2}) \quad . \tag{5.7}$$

From Fig. 2 we recall that the ratio ℓ_{ia_2}/ℓ_{ii_2} is very small and $\varepsilon \ell_{ia_2}/\ell_{ii_2}$ is even much smaller. The ion slip is indeed negligible.

Equation (4.13) yields two different equations, one on each side of the discontinuity. Near the point m(m = 1,2) we have

$$\frac{3}{2}\frac{dT_e}{dx^*} - f\frac{d}{dx^*}\left(\frac{T_e^{1/2}}{F_e}\frac{dT_e}{dx^*}\right) = -\frac{bT_e^{1/2}}{u_m^2}(T_e - T_m)\left[Q_{ee} + \frac{\ell_{ii_2}}{\ell_{ea_2}}Q_{ea}\right] . \tag{5.8}$$

Equations (4.10), (4.9), and (4.16) determine respectively the electric field, the charge separation and the potential by the relations

$$E = -\frac{\varepsilon\lambda_{D_2}}{\ell_{ii_2}}\frac{dT_e}{dx^*} , \tag{5.9}$$

$$\delta = \frac{\varepsilon\lambda_{D_2}}{\ell_{ii_2}}\frac{dE}{dx^*} , \tag{5.10}$$

$$\phi = T_e - T_1 . \tag{5.11}$$

We now split each of Eqs. (5.8) into two first order differential equations suitable for numerical integration. The result is

$$\frac{dT_e}{dx^*} = \frac{zF_e}{T_e^{1/2}} , \tag{5.12}$$

$$f\frac{dz}{dx^*} = \frac{3}{2}\frac{dT_e}{dx^*} + b\frac{T_e^{1/2}}{u_m^2}(T_e - T_m)\,G , \tag{5.13}$$

where

$$G = Q_{ee} + \frac{\ell_{ii_2}}{\ell_{ea_2}} Q_{ea} \quad . \tag{5.14}$$

The independent variable x^* is next eliminated by dividing Eqs. (5.13) by Eq. (5.12). The resulting direction field equation $\frac{dz}{dT_e} = f(z, T_e)$ is integrated numerically between points 1 and 2 to give a relation $z = z(T_e)$. With z known, the electron temperature distribution $T_e(x^*)$ can be found by integrating Eq. (5.12) where the origin of x^* is taken at a point such that $T_e = T_1 + 10^{-3}$. The electric field, charge separation and potential distributions are computed respectively from Eqs. (5.9), (5.10), and (5.11).

The upstream and downstream points 1 and 2 are obviously singular points of the system of Eqs. (5.12) and (5.13) and the direction field equation at these points is given by the ratio of two vanishing gradients. It is therefore necessary to determine the nature of the solution in the neighborhood of the singular points by a suitable linearization. Since at the singular points ($m = 1,2$) $T_e = T_m$ and $z = 0$, we assume that in the neighborhood of the singular points the solution is of the form

$$T_e = T_m + Ae^{kx^*} \quad , \quad z = Be^{kx^*} \quad , \tag{5.15}$$

where A and B are assumed to be small. On inserting these assumed forms of the solutions in Eqs. (5.12) and (5.13) and retaining

only those terms linear in A and B, one obtains a homogeneous system for A and B. The condition for the existence of a non-trivial solution is given by the characteristic equation. The nature of the roots of the characteristic equation, here a quadratic equation in k, determines the nature of the singular points. The slope of the characteristic direction, dz/dT_e, at these points is simply B/A.

At the singular points m = 1,2 the characteristic equations of the system of Eqs. (5.12) and (5.13) are

$$fk^2 - \frac{3}{2} F_{e_m} \frac{k}{T_m^{1/2}} - \frac{bT_m^{1/2}}{u_m^2} G_m F_{e_m} = 0 \quad , \tag{5.16}$$

where F_{e_m} and G_m denote the values of F_e and G at point m. Equations (5.16) always have two roots of opposite sign. It follows that points 1 and 2 are saddle points and the characteristic directions are given by the relation

$$\frac{dz}{dT_e} = \frac{k_m T_m^{1/2}}{F_{e_m}} \quad , \tag{5.17}$$

where k_1 is the positive root and k_2 the negative one of the respective characteristic equations. The integral curves obtained by integrating the direction field equation from points 1 and 2 successively are sketched in Fig. 3.

It has been pointed out that there is a discontinuity in the transition from point 1 to point 2. This discontinuity is represented in Fig. 3 by the line 3-4, where point 3 lies on the integral curve leaving point 1 at $x' \to -\infty$ and point 4 is on the integral curve reaching point 2 at $x' \to +\infty$. It will be seen that this discontinuity corresponds to an atom shock of thickness $\ell_{aa_2} << \ell_{ii_2}/\varepsilon$ in which the ion velocity and temperature jump from their upstream to their downstream values but where the electron temperature can be considered as constant. In particular we have

$$T_{e_3} = T_{e_4} \quad . \tag{5.18}$$

Integrating Eq. (4.13) with respect to x^* between points 4 and 3 with the assumption of constant electron temperature we obtain the following equation

$$f(z_3 - z_4) = T_{e_3} \log_e u_1 + b \int_{x_4^*}^{x_3^*} (T_{e_3} - 1)\, T_{e_3}^{1/2}\, G\, dx^* \quad . \tag{5.19}$$

The function G depends very weakly on the ion velocity and may be regarded as constant. Since the shock thickness is thin, $x_3^* \approx x_4^*$ and the integral on the right hand side of Eq. (5.19) vanishes. The relation between the coordinate z of points 3 and 4 becomes

$$z_3 - z_4 = \frac{T_{e_3}}{f} \log_e u_1 \quad . \tag{5.20}$$

For each point of the integral curve 2-4 we compute the corresponding point 3 from Eq. (5.20) to get the locus of point 3. The intersection of this locus and of the integral curve 1-3 determines the actual point 3. The solution is unique.

The electron temperature, electric field and potential distributions in the thermal layer are plotted in Fig. 4 and 5 for $M_1 = 3$ $T_1 = 10^4$ ^oK, $M_1 = 10$ $T_1 = 10^3$ ^oK, respectively and $\alpha = 10^{-3}$, $n_{a_1} = 10^{15}$ cm^{-3} in both cases. They are similar to the corresponding distributions obtained in the fully ionized case[1]. Due to the high electron thermal conductivity, the electron temperature rises to reach a value close to its downstream value at the atom shock. Because of the low degree of ionization the atom gas is essentially unaffected by the electrons and remains in its upstream state ahead of the shock front. In fact, the electrons are heated up by a very small decrease of ion-atom kinetic energy which is here negligible but which is appreciable for higher values of α. The ion flow is to a very good approximation in equilibrium with the atom flow. At $M_1 = 3$ the electron temperature rises slowly at first and then more and more rapidly near the shock. At $M_1 = 10$ on the contrary, the electron temperature rises sharply at the very beginning and more slowly afterwards. After the shock, the electron temperature reaches its downstream value slowly through collisions with the

atoms and ions. The thickness of the thermal layer varies from $3\ell_{ii_2}/\varepsilon$ at $M_1 = 1.5$ to $0.75\,\ell_{ii_2}/\varepsilon$ at $M_1 = 10$.

The electric field reflects the behavior of the electron temperature distribution since it is proportional to its gradient. It is always negative and for high Mach numbers exhibits a sharp single oscillation at the beginning of the thermal layer as a correlary to the sharp rise in T_e. It is precisely the same precursor electric shock layer which has been discussed in the fully ionized case[1]. Its thickness is $M_1\ell_{ii_1}/\varepsilon \ll \ell_{ii_2}/\varepsilon$. The potential distribution is identical to the electron temperature distribution except for the potential jump across the shock.

The atom shock structure equations are obtained now by setting $\Delta_s = \ell_{aa_2}$, replacing x_s by $x = x'/\ell_{aa_2}$ and neglecting terms of order α and ε. Equations (4.13), (4.12), (4.15), (4.11), (4.13), (4.10), (4.9), and (4.16) yield respectively the following equations:

$$\frac{dT_e}{dx} = O\left(\varepsilon \frac{\ell_{aa_2}}{\ell_{ii_2}}\right) \approx 0, \tag{5.21}$$

(hence T_e = constant = T_{e_3})

$$c\,\frac{T_a^{1/2}}{Q_{aa}}\,\frac{du_a}{dx} = \frac{5}{3}\,M_2^2(u_a - 1) + \frac{T_a}{u_a} - 1 \quad , \tag{5.22}$$

$$d\,\frac{T_a^{1/2}}{Q_{aa}}\,\frac{dT_a}{dx} = \frac{5}{6}\,M_2^2(u_a^2 - 1) + \frac{5}{2}\,(T_a - 1) - cu_a\,\frac{T_a^{1/2}}{Q_{aa}}\,\frac{du_a}{dx} \quad , \tag{5.23}$$

$$u_i = u_a - \frac{2}{a}\frac{\ell_{ia_2}}{\ell_{aa_2}}\frac{u_i u_a}{Q_{ia}(T_a + T_i)^{1/2}}$$

$$\left[\frac{du_i}{dx}\left(\frac{5}{3}M_2^2 - \frac{T_i + T_{e_3}}{u_i^2}\right) + \frac{1}{u_i}\frac{dT_i}{dx} - c\frac{\ell_{ia_2}}{\ell_{aa_2}}\frac{d}{dx}\left(\frac{T_i^{1/2}}{F_i}\frac{du_i}{dx}\right)\right] , \tag{5.24}$$

$$T_i = T_a - \frac{5}{9}M_2^2 u_a(u_i - u_a) - \frac{4\ell_{ia_2}}{b\ell_{aa_2}}\frac{u_i u_a}{Q_{ia}(T_i + T_a)^{1/2}}$$

$$\left[\frac{3}{2}\frac{dT_i}{dx} + \frac{T_i}{u_i}\frac{du_i}{dx} - \frac{\ell_{ia_2}}{\ell_{aa_2}}\left(c\frac{T_i^{1/2}}{F_i}\left(\frac{du_i}{dx}\right)^2 + d\frac{d}{dx}\left(\frac{T_i^{1/2}}{F_i}\frac{dT_i}{dx}\right)\right)\right] , \tag{5.25}$$

$$E = \frac{\lambda_{D_2}}{\ell_{aa_2}}\frac{T_{e_3}}{u_i}\frac{du_i}{dx} , \tag{5.26}$$

$$\delta = \frac{\lambda_{D_2}}{\ell_{aa_2}}\frac{dE}{dx} , \tag{5.27}$$

$$\phi = -T_{e_3}\log_e\left(\frac{u_i}{u_1}\right) + \phi_3 . \tag{5.28}$$

Equations (5.22) and (5.23) are the Navier-Stokes equations for a neutral gas whose solution for the velocity and temperature distributions is well known[17]. Since $\ell_{ia_2}/\ell_{aa_2} \ll 1$ Eqs. (5.24)

17. D. Gilbarg and D. Paolucci, J. Rat. Mech. and Anal. 2, 617, (1953).

and (5.25) show that to a good approximation, $u_i = u_a$ and $T_i = T_a$ except at the beginning of strong shocks where the dimensionless temperatures are very small. Equation (5.28) shows that the electrons in thermal equilibrium obey a Boltzmann distribution

$$n'_e = n'_{e_3} \exp\left[e(\phi' - \phi'_3)/kT'_{e_3}\right] \quad .$$

The atom velocity and temperature distributions are obtained by solving the system of Eqs. (5.22) and (5.23) according to the procedure used earlier to integrate the electron temperature distribution. Points 3 and 4 are singular points of this system and the characteristic equation at point 4 is:

$$dck^2 + k[d(1 - \frac{5}{3} M_2^2) - \frac{3}{2} c] + \frac{5}{2} (M_2^2 - 1) = 0 \quad . \qquad (5.29)$$

Since $M_2 < 1$, Eq. (5.29) has two roots of opposite sign. Point 4 is a saddle point. The characteristic direction of the integral curve in the $T_a - u_a$ plane is given by

$$(\frac{dT_a}{du_a})_4 = \frac{1}{dk - \frac{3}{2}} \quad , \qquad (5.30)$$

where k is the negative root of Eq. (5.29).

The characteristic equation at point 3 is deduced from Eq. (5.29) by replacing M_2 by M_1 in the parameters. Since $M_1 > 1$, it is easy to verify that the characteristic equation at point 3 has 2 positive roots and point 3 is a node.

There is only one integral curve passing through the saddle point 4 with the characteristic direction given by Eq. (5.30), while the node 3 is a center of attraction for all integral curves passing in its neighborhood. Therefore, the numerical integration is performed from point 4 towards point 3 and the origin of x is chosen at an arbitrary point near point 4.

When the ion slip is small the ion velocity and temperature distributions are assumed to be given by the following expansions in the small parameter ℓ_{ia_2}/ℓ_{aa_2}

$$u_i = u_a + \frac{\ell_{ia_2}}{\ell_{aa_2}} u_{i_1} + \ldots$$

$$T_i = T_a + \frac{\ell_{ia_2}}{\ell_{aa_2}} T_{i_1} + \ldots \qquad (5.31)$$

The terms $u_{i_1} \ldots, T_{i_1} \ldots$ are computed by substituting the expansions (5.31) in Eqs. (5.24) and (5.25) and identifying the terms of the same order in ℓ_{ia_2}/ℓ_{aa_2}. The first order terms are

$$u_{i_1} = -\frac{2u_a^2}{aQ_{ia}(2T_a)^{1/2}} \left[\frac{du_a}{dx}\left(\frac{5}{3}M_2^2 - \frac{T_a + T_e}{u_a^2}\right) + \frac{1}{u_a}\frac{dT_a}{dx}\right], \qquad (5.32)$$

$$T_{i_1} = -\frac{5}{9}M_2^2 u_a u_{i_1} - \frac{4u_a^2}{bQ_{ia}(2T_a)^{1/2}}\left[\frac{3}{2}\frac{dT_a}{dx} + \frac{T_a}{u_a}\frac{du_a}{dx}\right] . \qquad (5.33)$$

We note that the first order approximation for u_i and T_i does not contain the effect of ion viscosity and thermal conduction which are very small.

The electric field, potential, velocity, and temperature distributions for atoms and ions are plotted in Figs. 6 and 7 for $M_1 = 3$ and 10 respectively. The atom flow, unaffected by the charged particles, undergoes a shock in which the dissipative mechanisms are the atom viscosity and thermal conduction. Because of the large atom-ion cross section, the ion flow follows closely the atom flow and goes through the same shock. The negative electric field induced by the charge separation slows down the ions so that the ion velocity, which is at first slightly larger than the atom velocity, then decreases more rapidly. The ion temperature increases faster than the atom temperature and the atom-ion equilibrium is reached at the end of the shock after a sufficient number of atom-ion collisions.

At $M_1 = 3$ the ion slip is small throughout the shock. At $M_1 = 10$, the ion slip is still small except at the beginning of the shock where the method of solution based on the expansions (5.31) fails, as may be seen on Fig. 7. No acceptable numerical solution for u_i and T_i in the neighborhood of point 3 has been found yet. Analytically, the solution fails because $T_a^{1/2}$ is very small near point 3 and the first order terms given by Eqs. (5.32) and (5.33) are large. A physical explanation might be that the local collision time proportional to $T^{-1/2}$ is much larger at the beginning of the shock than at the end because of the high temperature ratio across the shock. As a result there are not enough ion-atom collisions at

the beginning of the shock to keep the ion slip small. A smaller value of the ratio ℓ_{ia_2}/ℓ_{aa_2} would improve the range of validity of our solution.

The electric field, always negative, shows a single symmetrical oscillation. The ratio R of the Coulomb force acting on the ions to the ion pressure gradient, defined by the relation

$$R = \frac{n_i' e \, |E_x'|}{\frac{dp_i'}{dx'}} \quad ,$$

increases through the shock from 0.4 to 0.8 for $M_1 = 10$. Therefore, there is an important coupling of the electrical effects with the ion flow.

The magnitudes of the shock thicknesses and of the electrical effects are given in Table 1 for typical plasma conditions at different Mach numbers. The thickness of the thermal layer ahead of the shock front is denoted by Δ_1. The shock thickness based on the maximum atom velocity gradient is denoted by Δ_2 and is given by

$$\Delta_2 = \frac{u_1 - 1}{\left(\frac{du_a}{dx}\right)_{max}} \quad .$$

As the Mach number increases the dimensionless electric field and the potential increase while the shock thickness increases. For different temperature and density conditions the electric field E_x' would vary as $n_a' T_1'^{3/4}$ and the potential rise as T_1'.

VI. PARTIALLY IONIZED PLASMA

We now consider in detail the case in which the degree of ionization α is no longer small. In this case the ionized particles have an important effect on the atom flow and the magnitude of this effect increases with the degree of ionization. We wish to investigate how the shock structure and the self-induced electric field vary with the upstream conditions and the degree of ionization. We shall compare the results obtained with the limiting case of a fully ionized plasma.

The shock structure is now investigated according to the method employed previously. We consider first the thermal layer of thickness $\Delta_s = \ell_{ii_2}/\varepsilon$ where x_s is replaced by $x^* = x'/\ell_{ii_2}$. Equations (5.6) and (5.7) still hold and we may set $u_i = u_a$, $T_i = T_a$ in the remaining shock equations. On neglecting those terms of order ε but retaining those of order α in Eqs. (4.12), (4.15), (4.13), (4.10), (4.9), and (4.16) respectively we obtain the following shock structure equations:

$$\frac{5}{3} M_2^2 (1 + \alpha)(u_a - 1) + \frac{T_a}{u_a} - 1 + \alpha\left(\frac{T_e}{u_a} - 1\right) = 0 , \quad (6.1)$$

$$\frac{2\alpha f T_e^{1/2}}{5F_e} \frac{dT_e}{dx^*} = \frac{M_2^2}{3}(1 + \alpha)(u_a^2 - 1) + T_a - 1 + \alpha(T_e - 1) , \quad (6.2)$$

$$f \frac{d}{dx^*}\left[\frac{T_e^{1/2}}{F_e} \frac{dT_e}{dx^*}\right] = \frac{3}{2} \frac{dT_e}{dx^*} + \frac{T_e}{u_a} \frac{du_a}{dx^*} + \frac{bT_e^{1/2}}{u_a^2}(T_e - T_a) G , \quad (6.3)$$

where G is defined by (5.14),

$$E = -\frac{\varepsilon\lambda_{D_2}}{\ell_{ii_2}} u_a \frac{d}{dx^*}\left(\frac{T_e}{u_a}\right) \quad , \tag{6.4}$$

$$\delta = \frac{\varepsilon\lambda_{D_2}}{\ell_{ii_2}} \frac{dE}{dx^*} \quad , \tag{6.5}$$

$$\phi = -\frac{\ell_{ii_2}}{\varepsilon\lambda_{D_2}} \int_1 E\, dx^* = \int_1 u_a d\left(\frac{T_e}{u_a}\right) \quad . \tag{6.6}$$

Equation (6.1) may be solved for T_a and the resulting relation used to eliminate T_a in Eq. (6.2) to give

$$f \frac{T_e^{1/2}}{F_e} \frac{dT_e}{dx^*} = \frac{10M_2^2(1+\alpha)}{3\alpha}(u_a - 1)(u_1 - u_a) \quad , \tag{6.7}$$

where $u_1 = (3 + M_2^2)/4M_2^2$.

Differentiating both sides of Eqs. (6.7) with respect to x^*, substracting the resulting equation from Eq. (6.3) and solving for $\frac{du_a}{dx^*}$ we obtain

$$\frac{du_a}{dx^*} = \left[\frac{3}{2}\frac{dT_e}{dx^*} + \frac{bT_e^{1/2}}{u_a^2}(T_e - T_a)G\right]\left[\frac{5(1+\alpha)}{2\alpha}\left(-\frac{8}{3}M_2^2 u_a + \frac{5}{3}M_2^2 + 1\right) - \frac{T_e}{u_a}\right]^{-} \tag{6.8}$$

Once T_a is eliminated in Eq. (6.8) with the aid of Eq. (6.1), Eqs. (6.7) and (6.8) form a set of two first order differential

equations in T_e and u_a. The method of solution is the same as that described earlier for the weakly ionized case. The variable x^* is eliminated by dividing Eq. (6.8) by Eq. (6.7) and the direction field equation $du_a/dT_e = f(T_e, u_a)$ is integrated between points 1 and 2 to give a relation $u_a = u_a(T_e)$. The electron temperature distribution $T_e(x^*)$ is obtained by integrating Eq. (6.7) and the ion temperature distribution, electric field, charge separation, potential are given in turn by Eqs. (6.1), (6.4), (6.5) and (6.6) respectively.

Points 1 and 2 are again singular points of Eqs. (6.7) and (6.8) and the characteristic equation at the points m = 1,2 is

$$\frac{fk^2}{F_{e_m}}\left(\frac{2\alpha}{5(1+\alpha)} - 1 + M_m^2\right) + k\left[\frac{3}{2}(1 - M_m^2) + \frac{2\alpha f b G_m}{5F_{e_m}}\left(\frac{5}{3}M_m^2 - 1\right)\right]$$

$$+ b\,G_m(1 - M_m^2)(1+\alpha) = 0 \quad . \tag{6.9}$$

The characteristic directions are

$$\frac{du_a}{dT_e} = \frac{2\alpha fk}{5(1+\alpha)F_{e_m}(1 - M_m^2)} \tag{6.10}$$

The product of the roots of Eq. (6.9) is of the sign of the expression $(1 - M_m^2)\left(\frac{2\alpha}{5(1+\alpha)} - 1 + M_m^2\right)$. At point 1, $M_1^2 > 1 > 1 - \frac{2\alpha}{5(1+\alpha)}$ and the product of the roots is negative, Eq. (6.9) has 2 roots of opposite sign and point 1 is a saddle

point. At point 2 two different situations arise: if $M_2^2 > 1 - \frac{2\alpha}{5(1+\alpha)}$ Eq. (6.9) has two negative roots and point 2 is a node. The minimum value of M_2 is reached at $\alpha = 1$ (fully ionized plasma) and corresponds to a maximum free stream Mach number of 1.12. This situation, therefore, corresponds to weak shocks. If $M_2^2 < 1 - \frac{2\alpha}{5(1+\alpha)}$, Eq. (6.9) has two roots of opposite sign and point 2 is a saddle point.

As in the fully ionized case[1] but in contrast to the weakly ionized case, for $\alpha \neq 0$ there are two different types of shock structure depending upon the Mach number. The particular "weak shock" solution cannot exist in the weakly ionized case because the condition $1 - \frac{2\alpha}{5(1+\alpha)} < M_2^2 < 1$ cannot be satisfied when $\alpha \gtrsim 0$.

In the weak shock case, when $M_2^2 > 1 - \frac{2\alpha}{5(1+\alpha)}$, the numerical integration is carried out from point 1 to point 2. The solution in the u_a, T_e phase space is continuous and has no extrema. The shock structure consists of a single relaxation layer. The results for $M_1 = 1.074$ at $\alpha = 0,7$ are plotted in Fig. 8. The shock thickness is so large (ℓ_{ii_2}/ϵ) that the atoms, ions, and electrons make many collisions and are in mechanical and thermal equilibrium through the shock.

When $M_2^2 < 1 - \frac{2\alpha}{5(1+\alpha)}$, the integral curve pattern in the u_a, T_e phase space is sketched in Fig. 9. The integral curve 1-3 leaving point 1 with the appropriate characteristic direction (corresponding to a positive root of Eq. (6.9)) has a maximum at

point 5 where it intersects the isocline of zero slope, a parabola whose equation is

$$T_e = \frac{5}{2\alpha}(1+\alpha)\, u_a\left(-\frac{8}{3}M_2^2 u_a + \frac{5}{3}M_2^2 + 1\right) \quad ,$$

and does not reach point 2 with the proper characteristic direction (corresponding to a negative root of Eq. (6.9)). Similarly, the integral curve 2-4 leaving point 2 with the appropriate direction does not reach point 1. There is no continuous integral curve joining points 1 and 2 and we must adopt the discontinuous solution 1-3-4-2. The discontinuity between points 3 and 4 represents a shock layer much thinner than the thermal layer which is investigated below.

We know that the shock thickness is of the order of ℓ_{aa_2} for a weakly ionized plasma and of the order of ℓ_{ii_2} for a fully ionized plasma. We may expect that, for intermediate values of the degree of ionization, the shock thickness is a function of the three mean free paths ℓ_{aa_2}, ℓ_{ii_2}, ℓ_{ia_2}. Considering the case in which α is small ($\lesssim 0.3$) we again set $\Delta_s = \ell_{aa_2}$. Eq. (4.15) gives:

$$\frac{dT_e}{dx} = O\left(\varepsilon \frac{\ell_{aa_2}}{\ell_{ii_2}}\right) \approx 0 \quad . \tag{6.11}$$

Hence, the electron temperature T_e may be considered as constant inside the shock and we set

$$T_e = T_{e_3} \quad . \tag{6.12}$$

On using Eq. (6.12), Eqs. (4.11) and (4.14) yield

$$u_i = u_a - \frac{2\,\ell_{ia_2}\,u_i u_a}{a\,\ell_{aa_2} Q_{ia}(T_a + T_i)^{1/2}} \left[\frac{du_i}{dx}\left(\frac{5}{3} M_2^2(1+\alpha) - \frac{T_i + T_{e_3}}{u_i^2}\right)\right.$$

$$\left. + \frac{1}{u_i}\frac{dT_i}{dx} - c\,\frac{\ell_{ia_2}}{\ell_{aa_2}}\frac{d}{dx}\left(\frac{T_i^{1/2}}{F_i}\frac{du_i}{dx}\right)\right] \quad , \tag{6.13}$$

$$T_i = T_a - \frac{5}{9} M_2^2(1+\alpha)\, u_a(u_i - u_a) - \frac{4\ell_{ia_2}\,u_i u_a}{b\ell_{aa_2} Q_{ia}(T_i + T_a)^{1/2}}$$

$$\left[\frac{3}{2}\frac{dT_i}{dx} + \frac{T_i}{u_i}\frac{du_i}{dx} - \frac{\ell_{ia_2}}{\ell_{aa_2}}\left(c\,\frac{T_i^{1/2}}{F_i}\left(\frac{du_i}{dx}\right)^2\right.\right.$$

$$\left.\left. + d\,\frac{d}{dx}\left(\frac{T_i^{1/2}}{F_i}\frac{dT_i}{dx}\right)\right)\right] \quad . \tag{6.14}$$

The ion slip is of the order of ℓ_{ia_2}/ℓ_{aa_2}, therefore small. It follows that, for α small, we may, to a good approximation replace u_i by u_a and T_i by T_a in Eq. (4.12) which becomes

$$cT_a^{1/2}\frac{du_a}{dx}\left(\frac{1-\alpha}{F_a} + \frac{\alpha\,\ell_{ia_2}}{F_i\,\ell_{aa_2}}\right) = \frac{5}{3} M_2^2(1+\alpha)(u_a - 1) + \frac{T_a}{u_a}$$

$$- 1 + \alpha\left(\frac{T_{e_3}}{u_a} - 1\right) \quad . \tag{6.15}$$

It is convenient at this point to replace Eq. (4.13) by the equation obtained by adding the atom and ion energy equations

(2.6) which, in dimensionless form, is written

$$dT_a^{1/2} \frac{dT_a}{dx} \left(\frac{1 - \alpha}{F_a} + \frac{\alpha \ell_{ia_2}}{F_i \ell_{aa_2}}\right) = - \frac{5}{6} M_2^2 (1 + \alpha) u_a^2$$

$$+ (1 + \alpha)\left(1 + \frac{5}{3} M_2^2\right) u_a + \frac{3}{2} T_a - \alpha T_{e_3} (1 + \log_e u_a) - F \quad . \tag{6.16}$$

The derivation of Eq. (6.16) is given in the Appendix B. The constant of integration F is determined at the boundary conditions at point 3 or 4.

The Hugoniot relations for the shock provide the boundary conditions at points 3 and 4 and are obtained by setting the derivatives in Eqs. (6.15) and (6.16) equal to zero. They are

$$\frac{5}{3} M_2^2 (1 + \alpha)(u_a - 1) + \frac{T_a}{u_a} - 1 + \alpha T_{e_3} = 0 \quad , \tag{6.17}$$

$$\frac{5}{6} M_2^2 (1 + \alpha) u_a^2 + \frac{5}{2} T_a - \alpha T_{e_3} \log_e u_a - F = 0 \quad . \tag{6.18}$$

The elimination of T_a between Eqs. (6.17) and (6.18) and of F computed at point 4 gives the "jump" condition satisfied by the velocity at point 3

$$5\left(\frac{5}{3} M_2^2 + 1\right)(u_a - u_4) - \frac{\alpha}{3} M_2^2 (u_a^2 - u_4^2) - \frac{2\alpha}{1 + \alpha} T_{e_3} \log_e \frac{u_a}{u_4} = 0 \quad . \tag{6.19}$$

If we put

$$y_1 = \frac{2\alpha}{1+\alpha} T_{e_3} \log_e \left(\frac{u_a}{u_4}\right)$$

and

$$y_2 = 5(u_a - u_4)\left[\left(\frac{5}{3} M_2^2 + 1\right) - \frac{4}{3} M_2^2 (u_a + u_4)\right] \quad ,$$

then from Fig. 10 it is clear that the equation $y_1 = y_2$, equivalent to Eq. (6.19), has only one root u_a other than $u_a = u_4$. For each point of the integral curve 2-4, we compute the corresponding point 3 from the jump condition (6.19) to get the locus of point 3. The intersection of this locus and of the integral curve 1-3 leaving point 1 determines the actual point 3. The solution is unique.

The structure equations (6.15) and (6.16) are integrated in the same way as the thermal layer equations. The characteristic equation at the singular points $m = 3,4$ obtained by setting $u_a = u_m + Ae^{kx}$, etc., is here

$$dc(1-\alpha)^2 \frac{T_m k^2}{F_{a_m}^2} - \frac{(1-\alpha) T_m^{1/2} k}{F_{a_m}} \left[d\left(\frac{5}{3} M_2^2 (1+\alpha) - \frac{T_m + \alpha T_{e_3}}{u_m^2}\right) + \frac{3}{2} c\right]$$

$$+ \frac{25}{6} M_2^2 (1+\alpha) - \frac{1+\alpha}{u_m}\left(\frac{5}{3} M_2^2 + 1\right) - \frac{(3T_m + \alpha T_{e_3})}{2u_m^2} = 0 \quad , \quad (6.20)$$

where F_{a_m} is the value of the function F_a at point m. Point 3 turns out to be a node and point 4 a saddle point. The atom

velocity and temperature distributions are obtained by integrating the direction field equation $dT_a/du_a = g(u_a, T_a)$ from point 4 to point 3.

The ion velocity and temperature distributions may not be given by the expansions (5.31) when the shock thickness is smaller than ℓ_{aa_2}. However, retaining the assumption of small ion slip we substitute u_a and T_a for u_i and T_i in the right hand side of Eqs. (6.13) and (6.14). This iterative method yields the following first order approximations for u_i and T_i:

$$u_i = u_a - \frac{2\ell_{ia_2} u_a^2}{a\ell_{aa_2} Q_{ia} (2T_a)^{1/2}} \left[\frac{du_a}{dx}\left(\frac{5}{3} M_2^2(1+\alpha) - \frac{T_a + T_{e_3}}{u_a^2}\right)\right.$$

$$\left. + \frac{1}{u_a}\frac{dT_a}{dx} - c\,\frac{\ell_{ia_2}}{\ell_{aa_2}}\frac{d}{dx}\left(\frac{T_a^{1/2}}{F_i}\frac{du_a}{dx}\right)\right] \qquad (6.21)$$

$$T_i = T_a - \frac{5}{9} M_2^2(1+\alpha)\, u_a(u_i - u_a) - \frac{4\ell_{ia_2} u_a^2}{b\ell_{aa_2} Q_{ia} (2T_a)^{1/2}} \left[\frac{3}{2}\frac{dT_a}{dx}\right.$$

$$\left. + \frac{T_a}{u_a}\frac{du_a}{dx} - \frac{\ell_{ia_2}}{\ell_{aa_2}}\left(c\,\frac{T_a^{1/2}}{F_j}\left(\frac{du_a}{dx}\right)^2 + d\,\frac{d}{dx}\left(\frac{T_a^{1/2}}{F_i}\frac{dT_a}{dx}\right)\right)\right] . \qquad (6.22)$$

It is found that the ion viscosity and thermal conduction appreciably reduce the ion slip and must be taken into account for $\alpha > 0.1$.

As in the weakly ionized case, the electric field, charge separation and potential are given respectively by Eqs. (5.26), (5.27), and (5.28).

Results for two different degrees of ionization $\alpha = 0.1$ and $\alpha = 0.5$ at a free stream Mach number $M_1 = 2$ are presented in Figs. 11 and 12 respectively. In contrast to the weakly ionized case, the atom shock retains some features of the ion shock in the fully ionized case[1].

In the thermal layer the electrons are heated up by the decrease in the kinetic energy of the flow, faster than the heavy particles, because of their higher thermal conductivity. When the degree of ionization becomes higher, the thermal energy of the electrons represents a larger fraction of the total energy and the velocity drop and the heating of atoms and ions increase.

The heating and the compression of the heavy particles occur, mainly in the shock layer where it can be seen that the atom and the ion temperatures overshoot their downstream values. Because of their much smaller mass the electrons do not have time in a few mean free paths to exchange energy with the heavy particles and the electron temperature is approximately constant through the shock.

The dissipative mechanisms in the shock are the viscosity and the thermal conduction of the ions and atoms. The ion slip is everywhere small for $\alpha = 0.1$; it is considerably larger for

$\alpha = 0.5$. Moreover it may be seen on Fig. 12 that the ion temperature and velocity distributions obtained from Eqs. (6.21) and (6.22) are locally in error at both ends of the shock where they overshoot their boundary values. In fact, for $\alpha = 0.5$ the solutions $u_a(x)$ and $T_a(x)$ obtained from Eqs. (6.15) and (6.16) do not represent the true atom velocity and temperature distributions but rather the average distributions for the whole plasma. This approximation may be responsible for the erroneous behavior of the ion velocity and temperature distributions at both ends of the shock. Unfortunately no acceptable numerical solution which permits a simultaneous calculation of the ion and atom velocity and temperature distributions has as yet been found.

The electric field varies slowly in the thermal layer and there is a single oscillation of negative amplitude in the shock. The potential reaches its maximum value at downstream infinity.

The shock structure for a strong shock ($M_1 = 10$) at $\alpha = 0.1$ is shown in Fig. 13. As in the weakly ionized case the electron temperature rises sharply at first and the electric field has a very sharp negative oscillation with a slower damping in the precursor electric shock layer at the beginning of the thermal layer. The ion slip is more important than at $M_1 \approx 2$ for the same degree of ionization and for the same reason as in the weakly ionized case the ion velocity and temperature distributions obtained from Eqs. (6.21) and (6.22) are in error near point 3. (The erroneous parts are drawn in dotted lines on Figs. 12 and 13.)

The variation of the shock thickness Δ_s and of the maximum electric field and potential with the degree of ionization α is given in Table II for $M_1 = 2$ and $M_1 = 10$. When α increases, the total number of atoms and ions being constant, the maximum electric field measured in V/cm increases, but since the shock thickness (measured in cm) decreases the potential rise across the shock stays constant for all degrees of ionization. The shock thickness is a minimum and the electric field is a maximum when the plasma is fully ionized. The shock thickness is smaller than the downstream atom-atom mean free path ℓ_{aa_2} for $\alpha > 0.2$ but is always much larger than the downstream ion-ion mean free path ℓ_{ii_2} except when $\alpha = 1$. The shock thickness decreases with the Mach number while the electric field and potential increase.

VII. CONCLUDING REMARKS AND COMPARISON WITH EXPERIMENT

The model that we have proposed covers in principle all plasma regimes from weakly to fully ionized. But unfortunately, the difficulty of numerically integrating more than two simultaneous differential equations between singular points requires that the solution be limited to an ionization less than about 30% so that, the ion slip s 's small throughout the shock.

Some feacures of the shock structure are common to all plasmas regimes such as the broad region of elevated electron temperature ahead of the shock front and the induced electric field which travels with the shock front. The potential rise across the shock is independent of the degree of ionization.

When the degree of ionization α varies from very low values to one, the shock strength decreases, and a partial compression and heating of the heavy particles occurs ahead of the shock front. The atom and ion temperatures overshoot their downstream values. The shock thickness, which is of the order of the downstream atom-atom mean free path when $\alpha << 1$ and of the order of the downstream ion-ion mean free path when $\alpha = 0(1)$, decreases continuously when α goes from zero to one.

The potential rise across the imbedded shock in a magnetic annular shock tube was measured by Heywood[18] in partially ionized hydrogen at a free stream temperature of $300^{\circ}K$, a molecular density of $8.75 \cdot 10^{15}$ cm^{-3} and a shock speed of 12.5 cm/μs. An electric probe, consisting of two steel electrodes separated by a distance of 0.6 cm and insulated from each other, was placed parallel to the axis of the shock tube, half way between the internal and external diameters. The electrodes were connected to the poles of an oscilloscope which measured the axial potential difference between them (voltage). The voltage distribution with time is shown on Fig. 14. As the travelling shock reaches the first electrode, the voltage, initially zero, increases to a sharp peak of 36V and decreases to zero again. The voltage variation occurs over a travel time corresponding to a distance of 1 cm. (The voltage increase on the right is due to the driving currents of magnetic origin and is irrelevant here.) This result shows that the shock

---

18. J. B. Heywood, Ph.D. Thesis, Department of Mechanical Engineering, M.I.T., Cambridge, September 1964. To be published.

thickness is at most equal to 1 cm although not smaller than the distance between the electrodes; were it otherwise, the voltage curve would have a flat maximum. Therefore in this case, the shock thickness is of the order of 0.6 cm, the distance between the electrodes. It may be possible in future experiments to evaluate the shock thickness more accurately by varying the distance between the electrodes. The maximum voltage occurs when the shock is exactly between the electrodes and represents the potential rise across the imbedded shock. For the conditions of the experiment, assuming that the dissociation is complete and 5% of the hydrogen is ionized, which corresponds to a free stream Mach number of 60, the theory predicts a shock thickness of 0.25 cm and a potential rise across the imbedded shock of 35V. The agreement with the measured potential rise of 36V is excellent, the agreement with the approximate measurement of the shock thickness is also good. These results suggest that the measurement of the potential rise may actually be a relatively simple method for the determination of shock thickness and the shock front location in shock tube experiments.

ACKNOWLEDGMENTS

This research has been supported by the Advanced Research Projects Agency (Ballistic Missile Defense Office) and technically administered by the Fluid Dynamics Branch of the Office of Naval Research under Contract Nonr-1841(93).

It is a great pleasure to thank Professor R. F. Probstein of the Massachusetts Institute of Technology for his interests in the problem and the careful reading of the manuscript. Thanks also go to John Heywood who provided the experimental data. The numerical computations were done at the Computation Center of M.I.T. and the author wishes to acknowledge the liberal amount of time allowed on a I.B.M. 7094 computer.

APPENDIX A

ATOM-ION ENERGY TRANSFER

Following Byron and Petschek[16] the ion-atom energy transfer per unit volume due to the random motion of the particles is

$$\Delta E = \frac{m_i}{2} n_i' n_a' \int (\vec{g} \cdot \vec{G})\, \sigma(g)\, g\, f_a f_i\, d\vec{c}_i d\vec{c}_a \quad , \qquad (A.1)$$

where $\vec{g}$ is the relative velocity in the mass center system, $\vec{G}$ the center of mass velocity, $\sigma(g)$ the cross section for ion-atom collisions, f_a and f_i are arbitrary normalized distribution functions and $\vec{c}_i$ and $\vec{c}_a$ the random particle velocities. The atom mass is taken equal to the ion mass m_i.

We choose $\vec{c}_a$ and $\vec{g}$ as variables of integration. According to the equations

$$\vec{c}_i = \vec{g} + \vec{c}_a \quad , \qquad (A.2)$$

$$d\vec{c}_i = d\vec{g} \quad , \qquad (A.3)$$

$$\vec{g} \cdot \vec{G} = \vec{g} \cdot \left(\frac{\vec{c}_a + \vec{c}_i}{2}\right) = \vec{c}_a \cdot \vec{g} + \frac{g^2}{2} \quad , \qquad (A.4)$$

Eq. (A.1) becomes

$$\Delta E = \frac{m_i}{2} n_i' n_a' \int \vec{c}_a \cdot \vec{g}\, \sigma(g)\, g\, f_a f_i\, d\vec{g}\, d\vec{c}_a + \frac{m_i}{4} n_i' n_a' \int g^3\, \sigma(g)\, f_a f_i\, d\vec{g}\, d\vec{c}_a \qquad (A.5)$$

Substituting into Eq. (A.5) the Maxwell distributions

$$f_a(\vec{c}_a) = \left(\frac{m_i}{2\pi k T'_a}\right)^{3/2} \exp\left(- m_i c_a^2/2kT'_a\right) \quad , \qquad (A.6)$$

$$f_i(\vec{c}_a + \vec{g}) = \left(\frac{m_i}{2\pi k T'_i}\right)^{3/2} \exp\left[- \frac{m_i}{2kT'_i} (c_a^2 + g^2 + 2\vec{c}_a \cdot \vec{g})\right] \quad , \qquad (A.7)$$

we obtain

$$\Delta E = \frac{m_i}{2} n'_i n'_a \left(\frac{m_i}{2\pi k \sqrt{T'_i T'_a}}\right)^3 \left\{\int \sigma(g)\, g \exp\left(- \frac{m_i g^2}{2kT'_i}\right) \int \vec{c}_a \cdot \vec{g} \exp\left[- \frac{m_i c_a^2}{2k} \left(\frac{1}{T'_i}\right.\right.\right.$$

$$\left.\left.\left. + \frac{1}{T'_a}\right) - m_i \vec{c}_a \cdot \vec{g}/kT'_i\right] d\vec{c}_a\, d\vec{g} + \frac{1}{2} \int g^3 \sigma(g) \exp\left(- \frac{m_i g^2}{2kT'_i}\right) \cdot\right.$$

$$\left. \cdot \int \exp\left[- \frac{m_i c_a^2}{2k} \left(\frac{1}{T'_i} + \frac{1}{T'_a}\right) - m_i \vec{c}_a \cdot \vec{g}/kT'_i\right] d\vec{c}_a\, d\vec{g}\right\} \qquad (A.8)$$

Integrating Eq. (A.8) with respect to the atom velocity and transforming the integration over the velocity $\vec{g}$ into an integration over the speed g we obtain

$$\Delta E = 2\pi m_i\, n'_a n'_i \left[\frac{m_i}{2\pi k (T'_a + T'_i)}\right]^{3/2} \left\{- \frac{T'_a}{T'_i + T'_a} \int_0^\infty g^5 \sigma(g) \exp\left[- \frac{m_i g^2}{2k(T'_i + T'_a)}\right] dg\right.$$

$$\left. + \frac{1}{2} \int_0^\infty g^5 \sigma(g) \exp\left[- \frac{m_i g^2}{2k(T'_i + T'_a)}\right] dg\right\}$$

$$= \frac{1}{\sqrt{\pi}\, (2k)^{3/2}} n'_a n'_i \left(\frac{m_i}{T'_a + T'_i}\right)^{5/2} (T'_i - T'_a) \int_0^\infty g^5 \sigma(g) \exp\left[- \frac{m_i g^2}{2k(T'_i + T'_a)}\right] dg \quad . \qquad (A.9)$$

Assuming that the cross section $\sigma(g)$ is independent of g as in the hard sphere model the integral term is easily computed and the result is

$$\Delta E = \frac{2\sqrt{2}}{\sqrt{\pi}} \left[\frac{k}{m_i}(T_i' + T_a')\right]^{1/2} Q_{ia}' n_i' n_a' k(T_i' - T_a') \quad , \quad (A.10)$$

where we have set $\sigma(g) = Q_{ia}'$.

The total energy transfer is the sum of the energy transfers due to the random and directed motions of the particles and is written

$$\xi_{ai} + u_a' P_{ai} = -2\left(\frac{2}{\pi}\right)^{1/2} n_a' n_i' \left[\frac{k}{m_i}(T_i' + T_a')\right]^{1/2} Q_{ia}' \left[k(T_a' - T_i') + \frac{(u_a' - u_i')}{3} m_i (u_a' + u_i')\right] \quad . \quad (A.11)$$

APPENDIX B

ION-ATOM ENERGY EQUATION

On adding the ion energy equation (2.6, $j = i$) to the atom energy equation (2.6, $j = a$), we obtain the following equation

$$m_i \frac{C_a}{2} \frac{du_a'^2}{dx'} + m_i \frac{C_i}{2} \frac{du_i'^2}{dx'} + \frac{5}{2} \frac{d}{dx'}(n_a' u_a' kT_a' + n_i' u_i' kT_i') - C_i eE_x'$$

$$- \frac{d}{dx'}(u_a' \mu_a'' \frac{du_a'}{dx'}) - \frac{d}{dx'}(u_i' \mu_i'' \frac{du_i'}{dx'}) - \frac{d}{dx'}(\kappa_a \frac{dT_a'}{dx'}) - \frac{d}{dx'}(\kappa_i \frac{dT_i'}{dx'})$$

$$= \xi_{ae} + u_a' P_{ae} + \xi_{ie} + u_i' P_{ie} \quad . \quad (B.1)$$

Inside the shock of thickness ℓ_{aa_2} or ℓ_{ii_2}, the momentum and energy transfer between the electrons and the heavy particles is negligible and the right hand side of Eq. (B.1) vanishes. Furthermore, inside the shock T_e' is constant and Eq. (2.10) yields

$$C_i\, eE_x' = \frac{C_i\, kT_e'}{u_i'} \frac{du_i'}{dx'} \quad . \tag{B.2}$$

On substituting $C_i eE_x'$ by its value from Eq. (B.2) in Eq. (3.1) and integrating with respect to x' when T_e' is constant, we obtain the following equation

$$\kappa_a \frac{dT_a'}{dx'} + u_a' \mu_a'' \frac{du_a'}{dx'} + \kappa_i \frac{dT_i'}{dx'} + u_i \mu_i'' \frac{du_i'}{dx'} = m_1 \frac{C_a}{2} u_a'^2$$

$$+ m_i \frac{C_1}{2} u_i'^2 + \frac{5}{2} k(C_a T_a' + C_i T_i') - C_i\, kT_e' \log_e u_i' - F' \quad , \tag{B.3}$$

which in dimensionless form may be written

$$\frac{\ell_{aa_2}\, T_a^{1/2}}{\Delta_s F_a} \left(d \frac{dT_a}{dx_s} + cu_a \frac{du_a}{dx_s}\right) + \frac{\alpha}{(1-\alpha)} \frac{T_i^{1/2}\, \ell_{ia_2}}{F_i \Delta_s} \left(d \frac{dT_i}{dx_s} + cu_i \frac{du_i}{dx_s}\right)$$

$$= \frac{5}{6} M_2^2 (1+\alpha)\left(u_a^2 + \frac{\alpha}{1-\alpha} u_i^2\right) + \frac{5}{2}\left(T_a + \frac{\alpha}{1-\alpha} T_i\right) - \frac{\alpha T_e}{1-\alpha} \Big] g_e\, u_a - F \tag{B.4}$$

In the shock we set $\Delta_s = \ell_{aa_2}$, $x_s = x$, $u_i = u_a$, $T_i = T_a$, $T_e = T_{e_3}$ and Eq. (B.4) becomes

$$\left(\frac{1-\alpha}{F_a} + \frac{\alpha \ell_{ia_2}}{F_i \ell_{aa_2}}\right)\left(c u_a T_a^{1/2} \frac{du_a}{dx} + d T_a^{1/2} \frac{dT_a}{dx}\right) = \frac{5}{6} M_2^2 (1+\alpha) u_a^2$$

$$+ \frac{5}{2} T_a - \alpha T_{e_2} \log_e u_a - F \quad . \qquad (B.5)$$

Multiplying Eq. (6.15) by u_i and subtracting from the above equation, we obtain Eq. (6.16).

M_1	T_1 °K	T_2 °K	$\frac{e\Delta_1}{\ell_{ii_2}}$	$\frac{\Delta_2}{\ell_{aa_2}}$	$\frac{\ell_{aa_2}}{\lambda_{D_2}} E_{max}$	$(\frac{\ell_{aa_2}}{\lambda_{D_2}})^2 \delta_{max}$	ϕ_{max}	$E'_{x_{max}}$ V/cm	ϕ'_{max} V	Δ_2 cm
1.5	10^4	1.5 10^4	1.663	10	-0.052	+0.009	.84	-.261	1.09	2.68
3	10^4	3.67 10^4	0.513	0.5	-0.17	+0.057	1.75	-12.8	5.55	1.25
10	10^3	3.21 10^4	0.265	5.5	-0.236	+0.096	2.22	-4.57	0.15	0.765

TABLE 1. Maximum magnitudes of electric field and charge separation, potential rise across shock and shock thicknesses as a function of free stream Mach number M_1 for a degree of ionization $\alpha = 10^{-3}$ and an atom number density $n_{a_1} = 10^{15}$ cm^{-3}.

Upstream Conditions	α	Δ_s/ℓ_{aa_2}	Δ_s/ℓ_{ii_2}	Δ_s cm	$\frac{\ell_{ii_2}}{\lambda_{D_2}} E_{max}$	$E'_{x_{max}}$ V/cm	ϕ_{max} V	ℓ_{aa_2}/ℓ_{ii_2}
$M_1 = 2$	0.1	2.9	15.4	0.724	$-4.62\ 10^{-2}$	-1.76	2.78	5.3
$T_1 = 10^4\ ^oK$	0.2	1.8	21.2	0.5	$-3.82\ 10^{-2}$	-2.92	2.275	11.8
$n_{a_1} + n_{i_1}$	0.5	0.44	20.9	0.196	$-5.26\ 10^{-2}$	-10.0	2.77	47.5
$= 10^{15}\ cm^{-3}$	1		6	$2.82\ 10^{-2}$	-0.100	-38.2	2.28	-
$M_1 = 10$	0.1	2.10	5.5	0.335	-.236	-10.7	5.95	2.62
$T_1 = 10^3\ ^oK$	0.2	1.38	8.1	0.247	-.210	-19.1	5.95	5.87
$n_{a_1} + n_{i_1}$	0.3	0.78	7.9	0.161	-.226	-30.8	5.95	10.1
$= 10^{15}\ cm^{-3}$	1		1.7	$1.04\ 10^{-2}$	-.421	-191	6.00	-

TABLE 2. Maximum magnitudes of electric field, potential rise across shock and shock thickness as a function of the degree of ionization α for moderate and strong shocks.

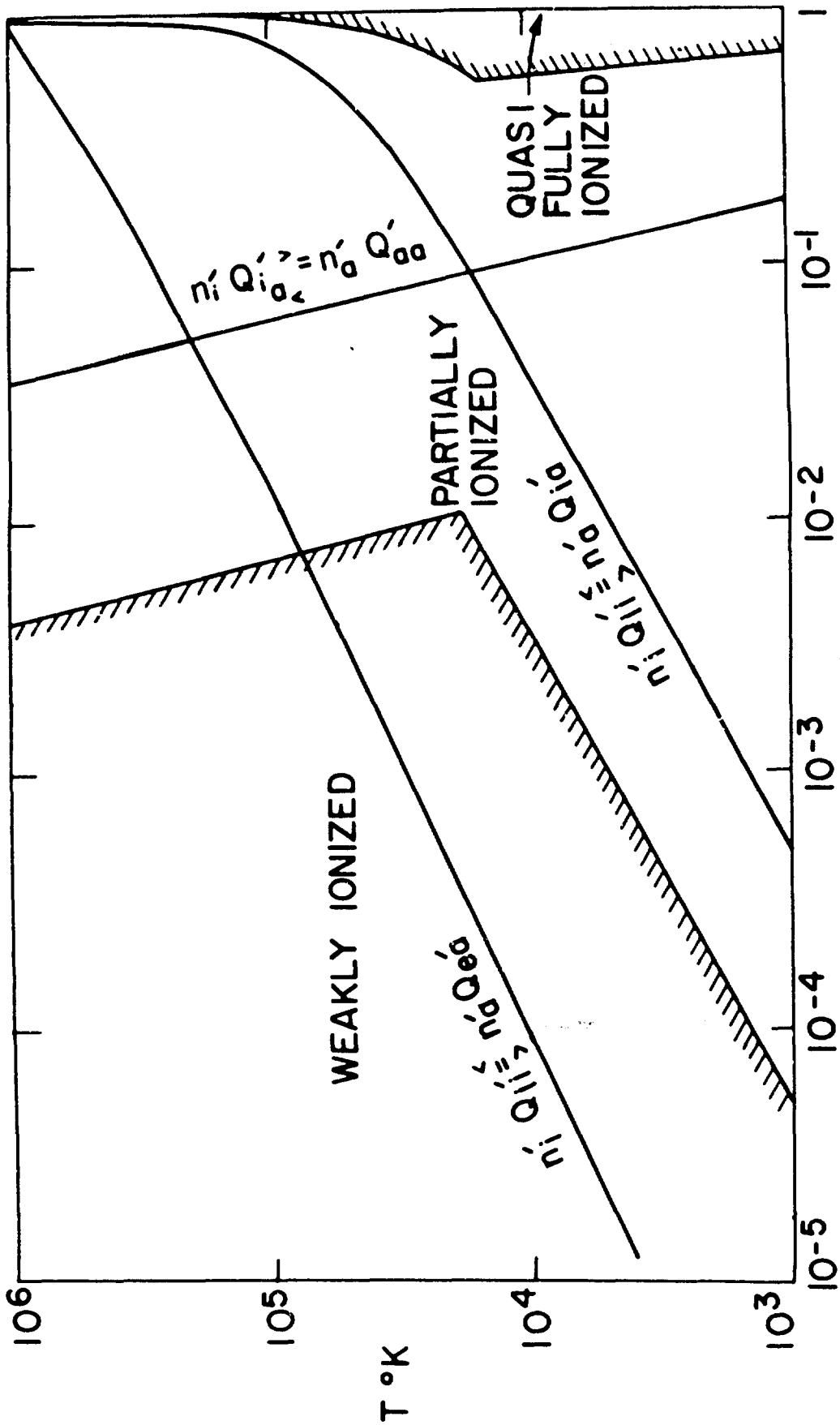

Fig. 1. Different plasma regimes for Argon (weakly ionized, $n'_i Q'_{ii} \leq 0.1\, n'_a Q'_{ia}$, $n'_i Q'_{ia} \leq 0.1\, n'_a Q'_{aa}$; quasi-fully ionized, $n'_i Q'_{ii} \geq 10\, n'_a Q'_{ia}$; $n'_i Q'_{in} \geq 10\, n'_a Q'_{aa}$).

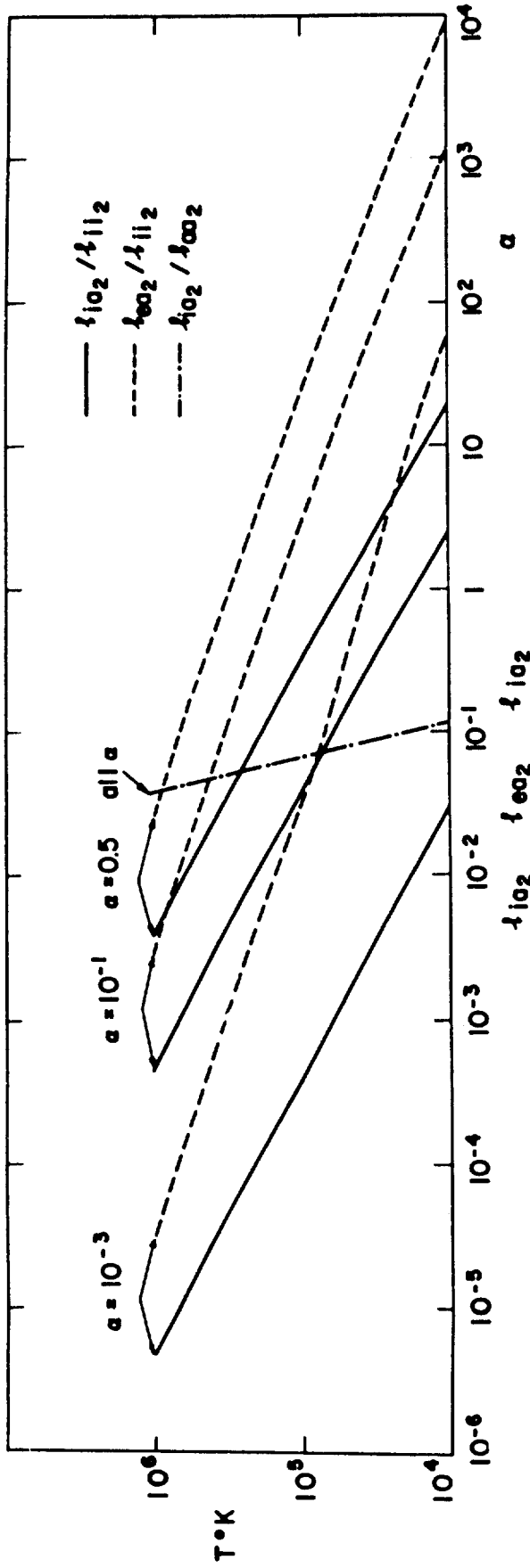

Fig. 2. Comparison of different mean free paths in Argon.

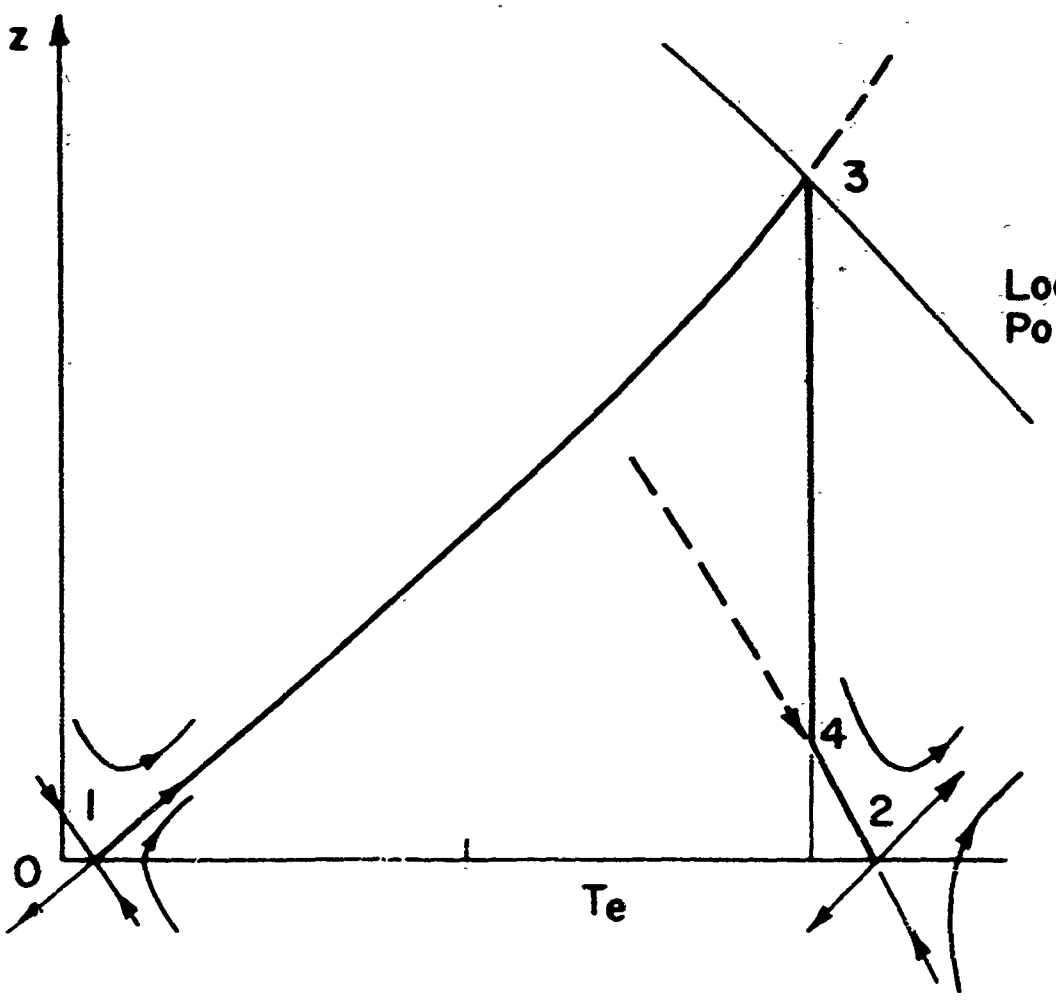

Fig. 3. Integral curves in z - T_e plane for weakly ionized plasma (arrows indicate direction of increasing x*).

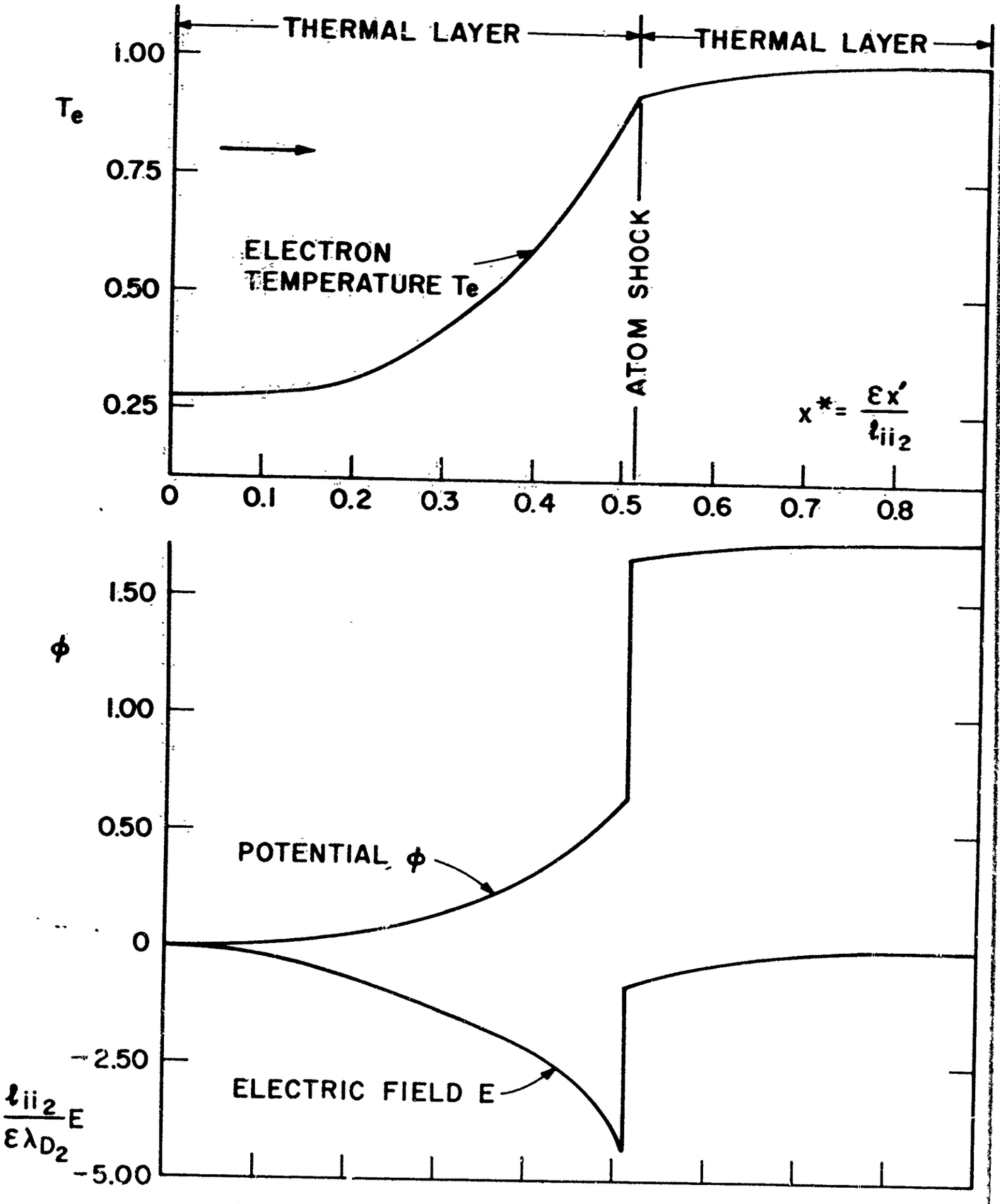

Fig. 4. Electron temperature, electric field and potential distributions in the thermal layer for the weakly ionized case ($\alpha = 10^{-3}$) at $M_1 = 3$.

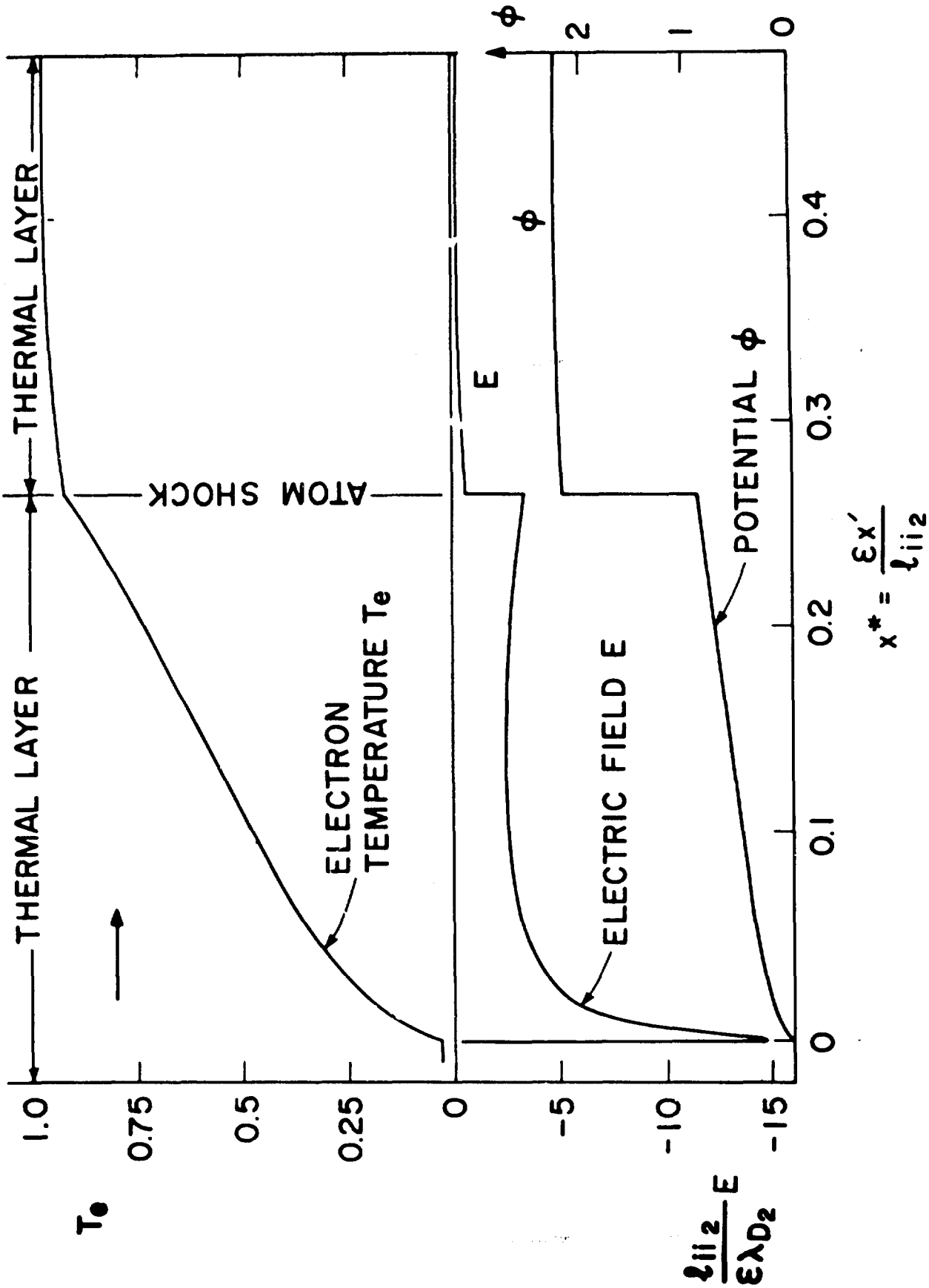

Fig. 5. Electron temperature, electric field and potential distributions in the thermal layer for the weakly ionized case ($\alpha = 10^{-3}$) at $M_1 = 10$.

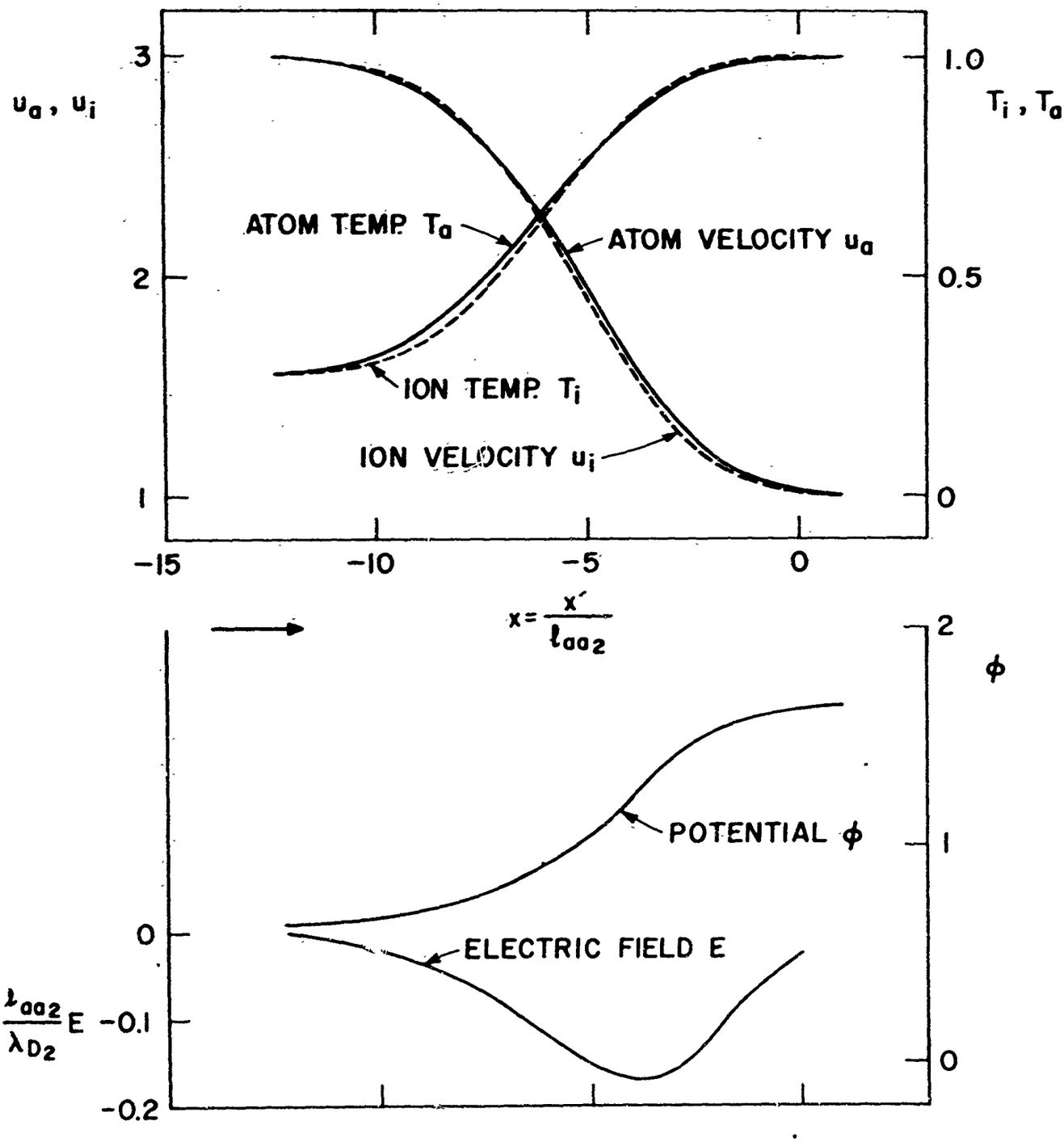

Fig. 6. Velocity, temperature, electric field and potential distributions in the atom shock for the weakly ionized case ($\alpha = 10^{-3}$) at $M_1 = 3$.

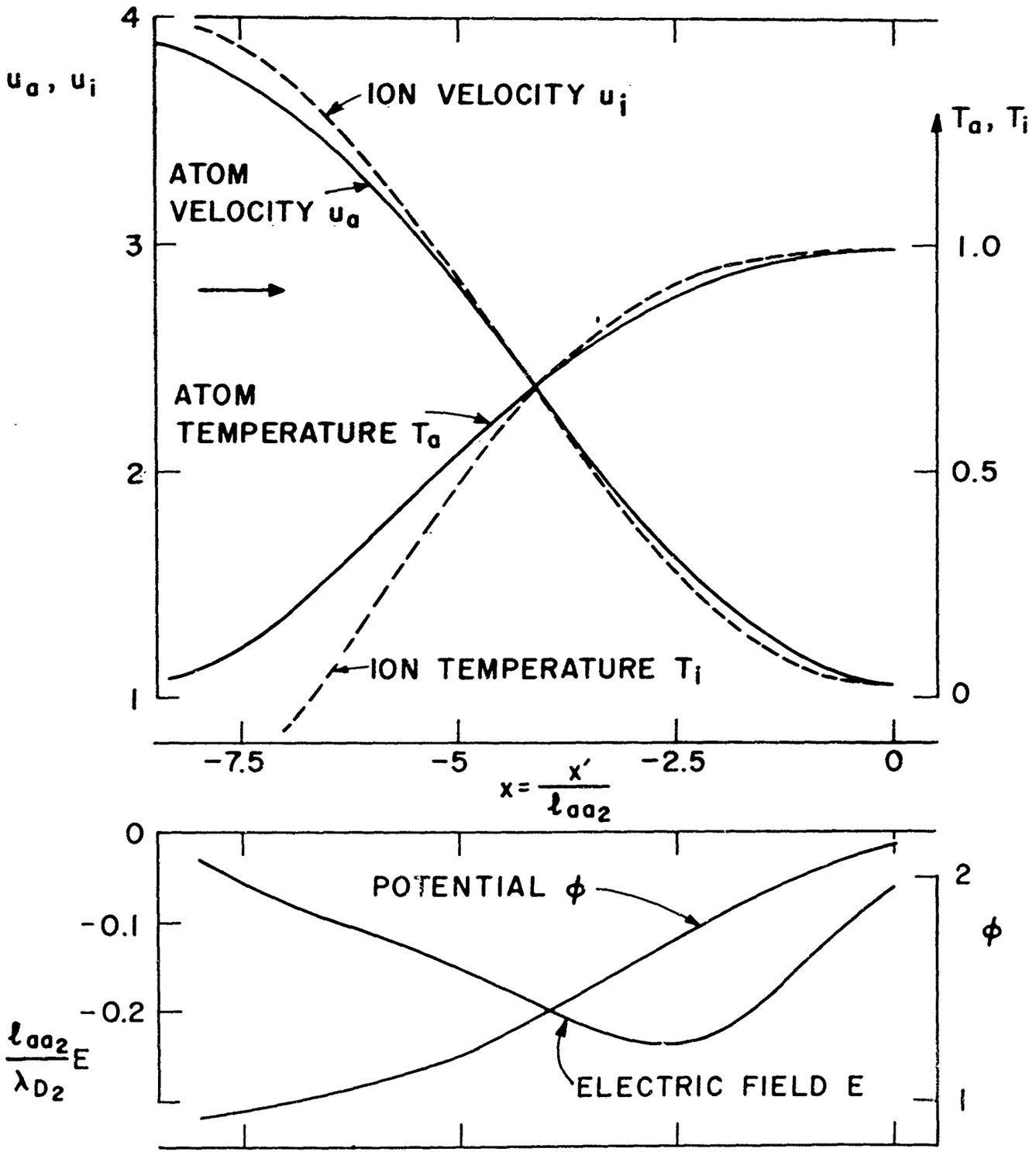

Fig. 7. Velocity, temperature, electric field and potential distributions in the atom shock for the weakly ionized case ($\alpha = 10^{-3}$) at $M_1 = 10$.

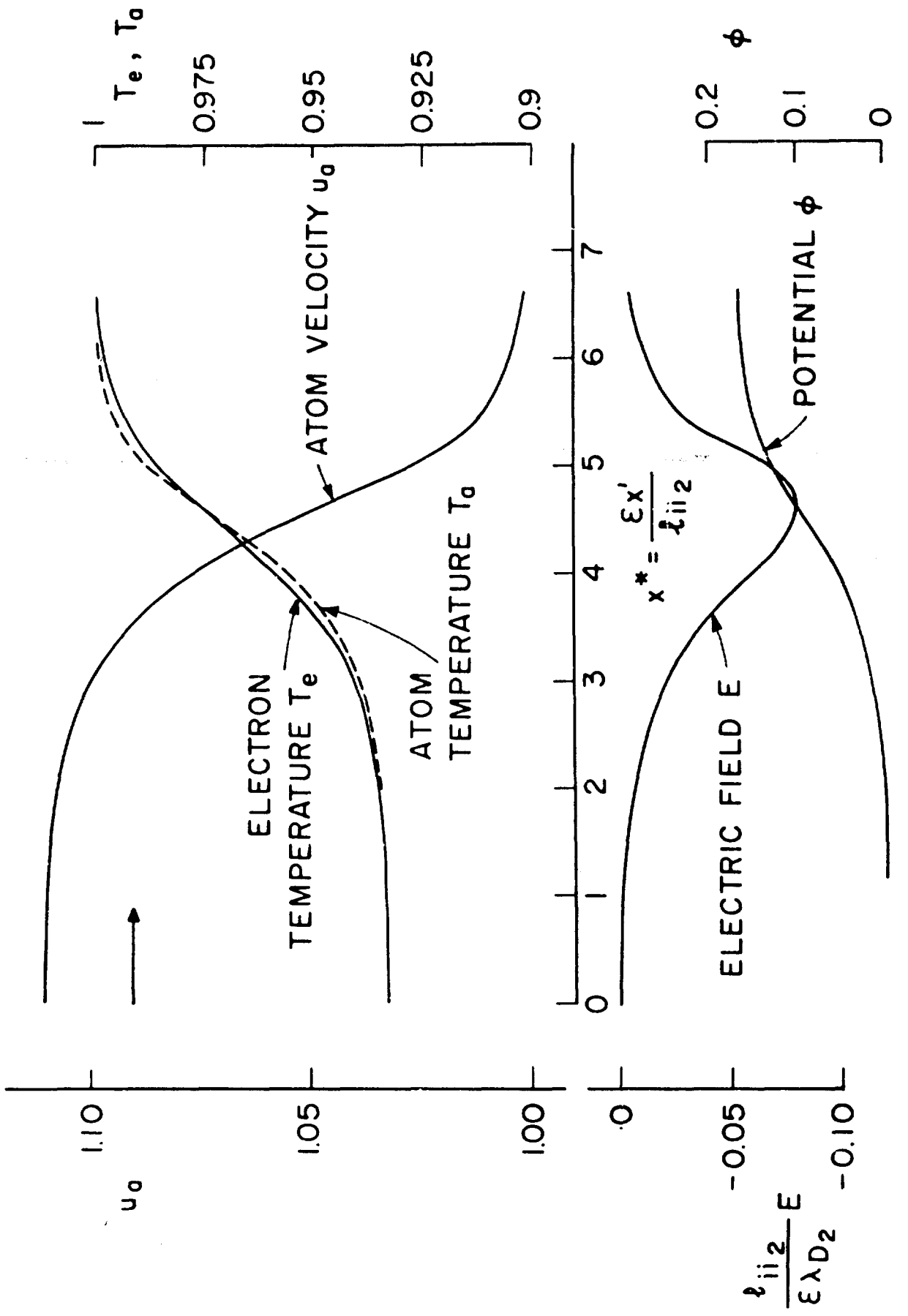

Fig. 8. Velocity, temperature, electric field and potential distributions through a weak shock ($M_1 = 1.074$) at $\alpha = 0.7$.

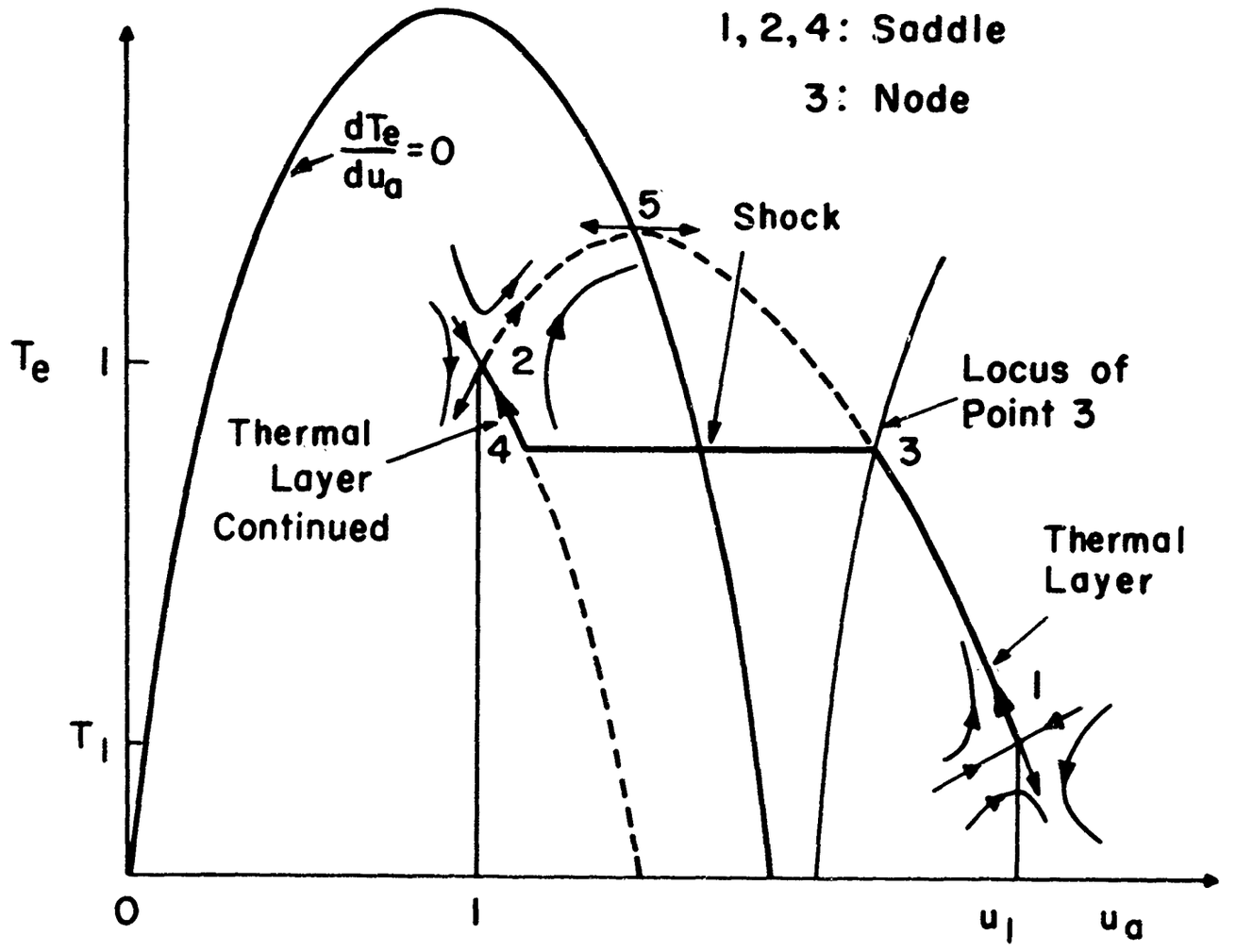

Fig. 9. Integral curves in $T_e - u_a$ phase space for moderate and strong shocks ($M_2^2 < 1 - \frac{2\alpha}{5(1+\alpha)}$).

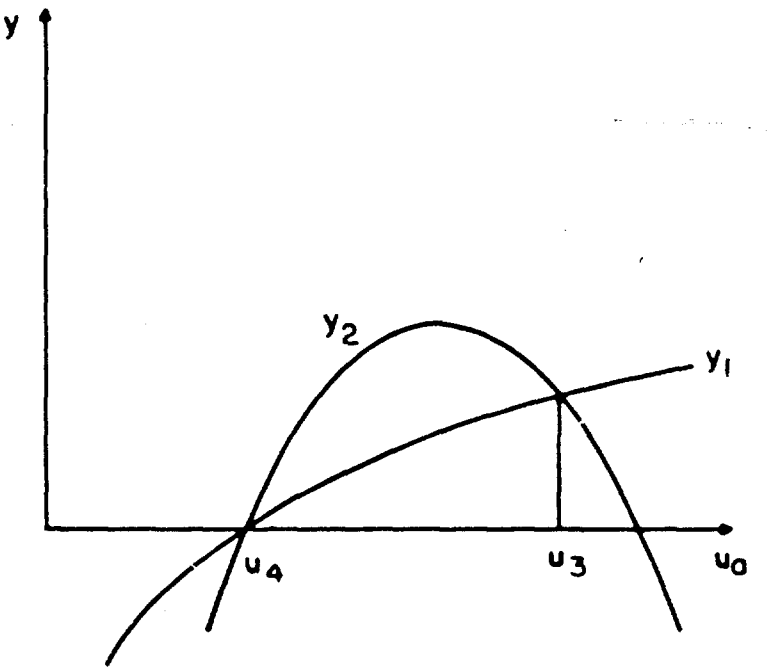

Fig. 10. Determination of the locus of points 3 defining beginning of imbedded shock for $M_2^2 < 1 - \frac{2a}{5(1+a)}$.

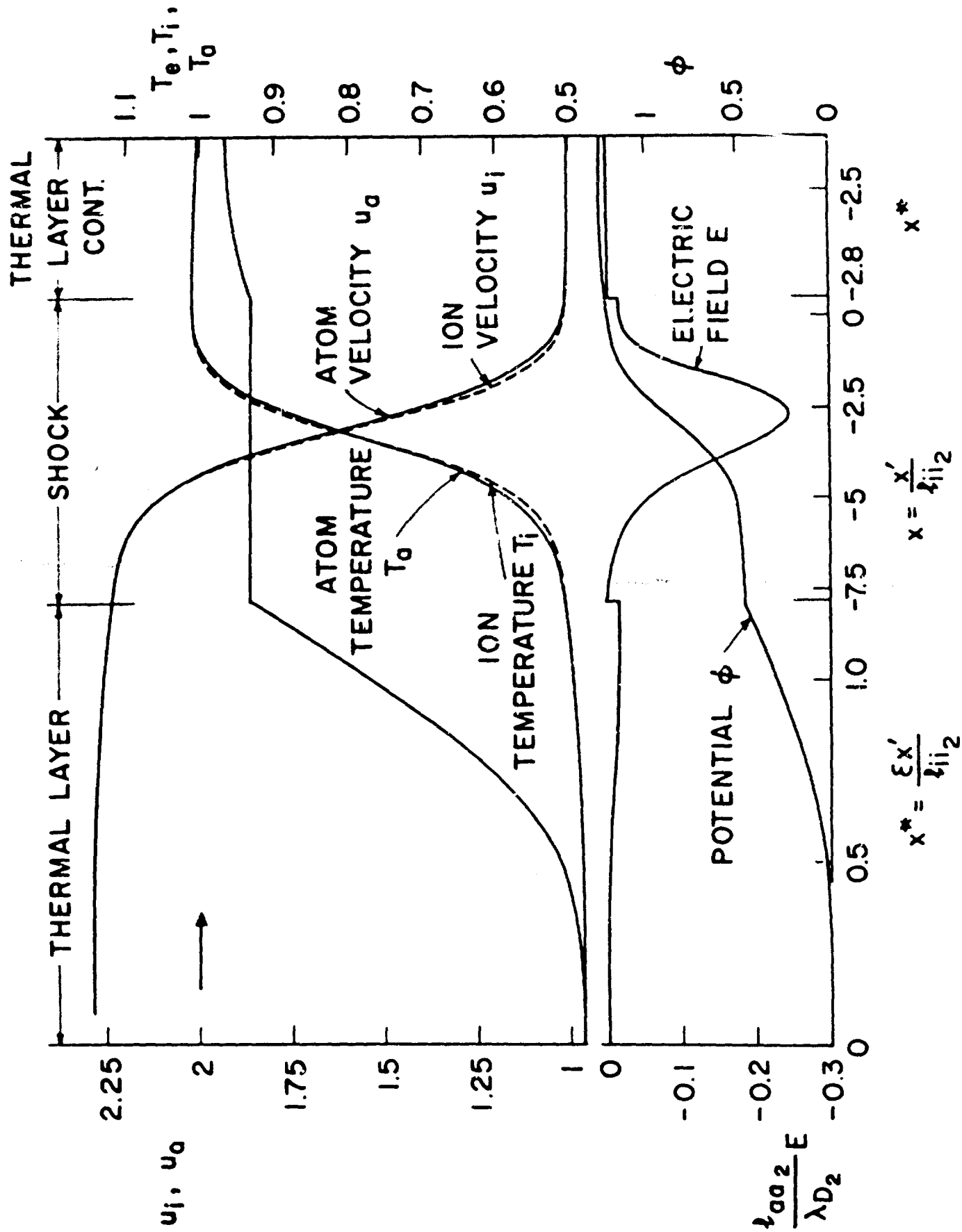

Fig. 11. Velocity, temperature, electric field and potential distributions through a moderate strength shock ($M_1 = 2$) at $\alpha = 0.1$.

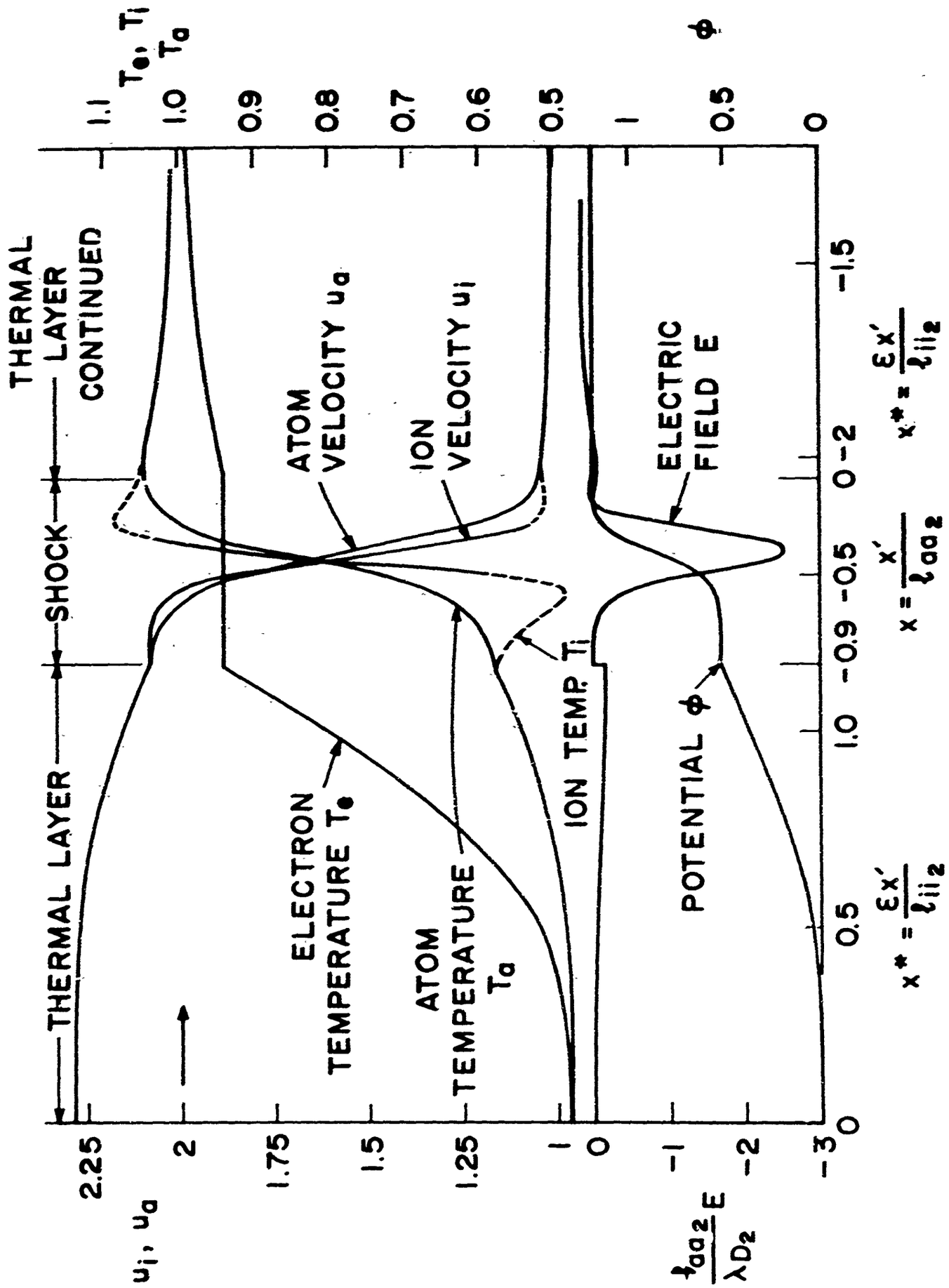

Fig. 12. Velocity, temperature, electric field and potential distributions through a moderate strength shock ($M_1 = 2$) at $\alpha = 0.5$.

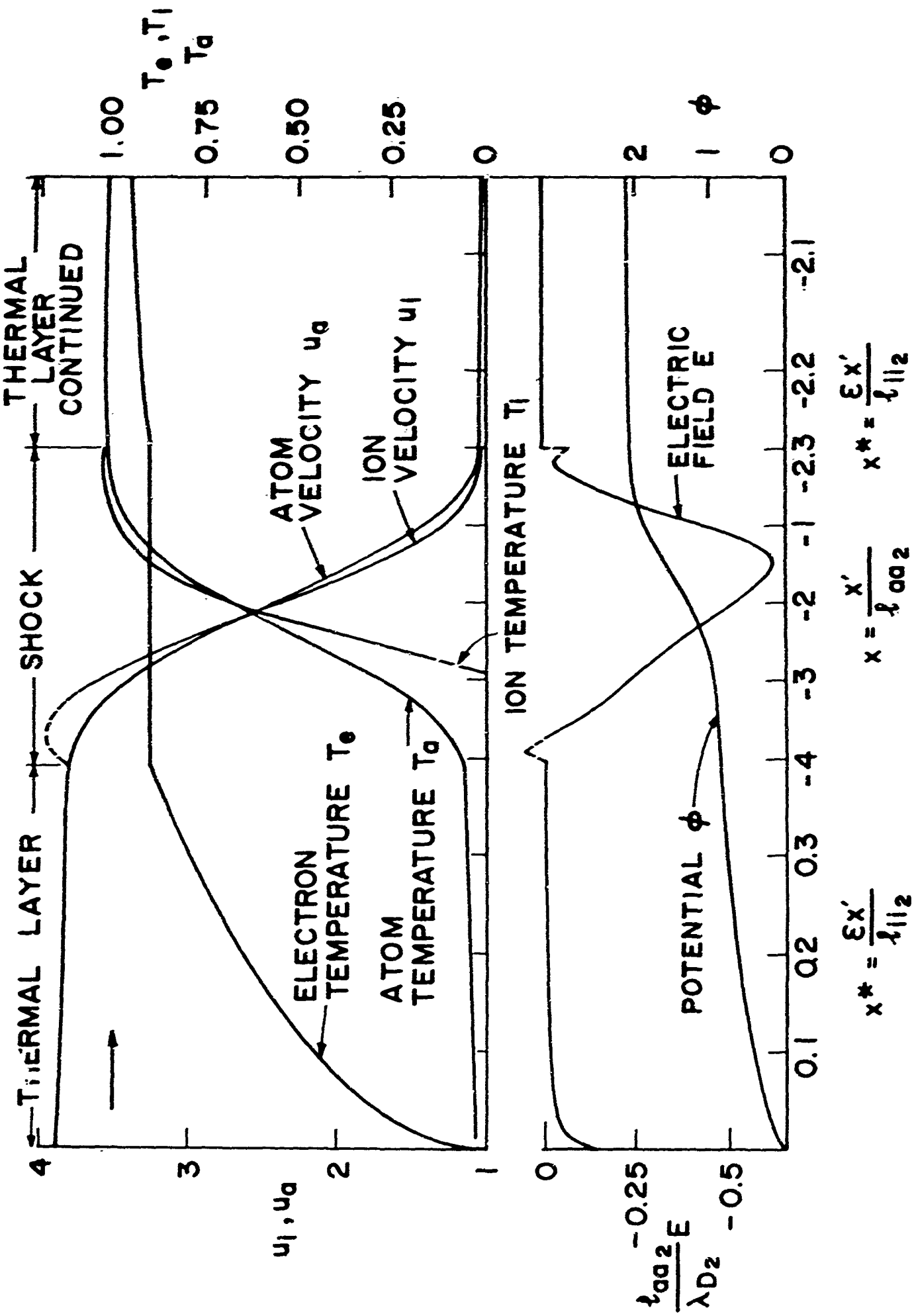

Fig. 13. Velocity, temperature, electric field and potential distributions through a strong shock ($M_1 = 10$) at $\alpha = 0.1$.

Fig. 14a. Voltage distribution as a function of time for a shock speed of 12.5 cm/μs, a free stream temperature of 300°K and a molecular density of $8.75 \cdot 10^{15}$ cm^{-3} in partially ionized hydrogen.

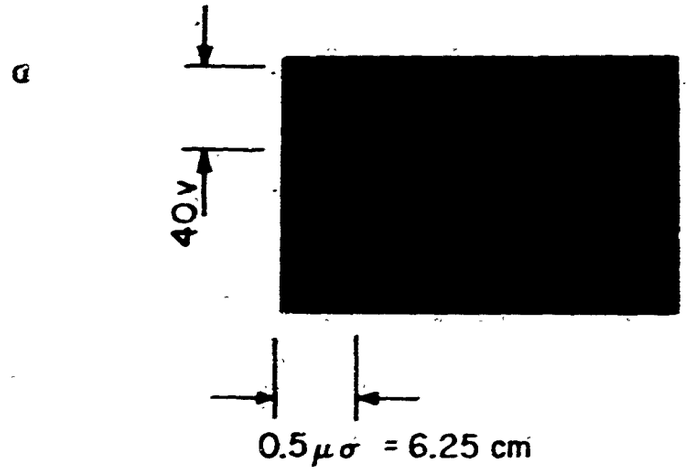

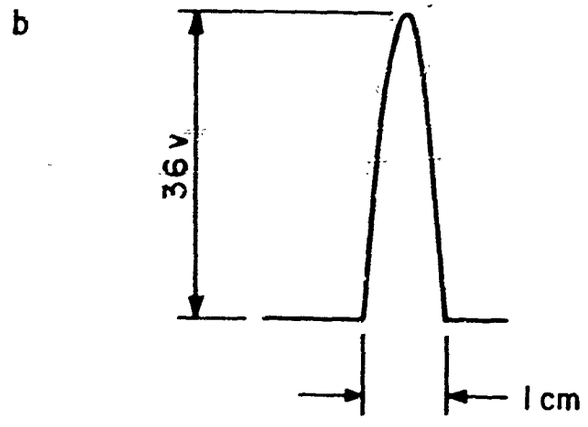

Fig. 14b. Detail of the region shown by the arrow in Fig. 14a corresponding to the potential rise across the imbedded shock.